High-throughput characterization of mutations in genes that drive clonal evolution using multiplex adaptome capture sequencing

Daniel E. Deatherage[1] and Jeffrey E. Barrick[1,2,*]

[1]Department of Molecular Biosciences, Center for Systems and Synthetic Biology, The University of Texas at Austin, Austin, TX 78712, USA

[2]Lead contact

[*]Correspondence: jbarrick@cm.utexas.edu

SUMMARY

Understanding how cells are likely to evolve can guide medical interventions and bioengineering efforts that must contend with unwanted mutations. The adaptome of a cell—the neighborhood of genetic changes that are most likely to drive adaptation in a given environment—can be mapped by tracking rare beneficial variants during the early stages of clonal evolution. We used multiplex adaptome capture sequencing (mAdCap-Seq), a procedure that combines unique molecular identifiers and hybridization-based enrichment, to characterize mutations in eight *Escherichia coli* genes known to be under selection in a laboratory environment. We tracked 301 mutations at frequencies as low as 0.01% and inferred the fitness effects of 240 of these mutations. There were distinct molecular signatures of selection on protein structure and function for the three genes with the most beneficial mutations. Our results demonstrate how mAdCap-Seq can be used to deeply profile a targeted portion of a cell's adaptome.

Keywords

Clonal interference, Distribution of fitness effects, Long-term evolution experiment with *E. coli* (LTEE), Pyruvate kinase, DNA Topisomerase I, PykF, NadR, TopA

INTRODUCTION

New mutations arise naturally in the genomes of cells during DNA replication and repair. These *de novo* mutations are the main drivers of adaptive evolution in clonal populations that have little or no recombination or standing genetic variation. For example, numerous lineages with different beneficial mutations arise and contend within large laboratory populations of asexual microbes before any one lineage outcompetes the ancestor and its competitors (Good et al., 2017; Lang et al., 2013; Maddamsetti et al., 2015). This 'clonal interference' leads to heterogeneous populations with many lineages simultaneously adapting via different sets of mutations (Desai et al., 2012; Gerrish and Lenski, 1998; Park and Krug, 2007). Often a majority of these mutations affect a small subset of genes involved in cellular processes that are under the strongest selection (Deatherage et al., 2017; Lang et al., 2013; Lind et al., 2015; Phaneuf et al., 2020). If the 'evolvome' is defined as the set of all spontaneous genetic changes by which a cell can potentially evolve, then the beneficial mutations that are most likely to drive adaptation in a given environment can be described as constituting its 'adaptome' (Ryall et al., 2012).

Human cancers and microbial infections exhibit similar genetic dynamics to those observed in these laboratory evolution experiments: single cells clonally expand as they evolve driver mutations that lead to disease progression and drug resistance. In cancer, both solid tumors and blood cancers have been shown to be genetically heterogeneous (Marusyk et al., 2012; Merlo et al., 2006; Thomas et al., 2006). *De novo* mutations that arise and then take over normal cell populations can lead to carcinogenesis (Genovese et al., 2014; Watson et al., 2020). Mutations in cancer cells drive neoplastic progression (Merlo et al., 2010), differences in responses to chemotherapy (Landau et al., 2013), and relapse (Ding et al., 2012). Similarly, populations of *Pseudomonas aeruginosa* and other bacteria that persistently infect the lungs of cystic fibrosis

patients become increasingly invasive and antibiotic resistant over time (Marvig et al., 2015; Stefani et al., 2017; Winstanley et al., 2016). In both cancers and infections, the same genes are often mutated in the cells that cause disease in different individuals. Mapping the adaptomes of these cells to understand how they are likely to evolve in other patients afflicted in the same way could inform treatment decisions and improve medical outcomes.

Cells used in biomanufacturing are also prone to evolving unwanted genetic heterogeneity (Renda et al., 2014; Rugbjerg and Sommer, 2019). Typically, these cells have been highly engineered to optimize the titer of a product of interest at the expense of rapid cellular replication (Lee and Kim, 2015; Nielsen and Keasling, 2016). Therefore, there are strong selective pressures for 'escape mutations' that cause production to decline. Usually escape mutations directly inactivate one or more key genes in the engineered pathway. The resulting nonproducing cells can become dominant during the many cell divisions that are necessary to scale these processes up to large bioreactors (Rugbjerg et al., 2018; Sandoval et al., 2014; Zelder and Hauer, 2000). Mapping the adaptomes of engineered cells to profile the evolutionary failure modes that are most common in nonproducing mutants before attempting scale-up could guide bioengineering design decisions and thereby improve the efficiency of industrial processes.

Evolution experiments conducted in laboratory environments reproduce key aspects of microbial evolution that are observed in chronic infections and bioreactors (Barrick and Lenski, 2013; Gresham and Dunham, 2014). Certain aspects of genomic and phenotypic evolution in these controlled systems predictably occur across multiple replicate populations (Barrick, 2020; Cvijović et al., 2018; Furusawa et al., 2018; McDonald, 2019; Rainey et al., 2017), making them a useful testbed for adaptome mapping methods. In theory, tracking the frequencies of mutations during the earliest stages of clonal evolution from a single cell in these populations should allow

one to map that cell's adaptome. However, many highly beneficial mutations arise but never reach appreciable frequencies in microbial populations before they are outcompeted by lineages with other beneficial mutations (Desai et al., 2012; Gerrish and Lenski, 1998). Thus, one must be able to track extremely rare mutations to recover more of the adaptome. During the initial burst of new beneficial genetic diversity when all beneficial mutations are still rare and very few cells have accumulated multiple mutations, each mutant is effectively competing only versus the ancestor. Therefore, one can also estimate each beneficial mutation's fitness effect directly from how rapidly its frequency increases during this critical time window.

High-throughput metagenomic DNA sequencing can be used to track rare mutations in cell populations, but most such studies of microbial evolution experiments have only been able to reliably identify mutations that are present at frequencies above ~1-10% due to limitations imposed by sequencing depth or error rates (Barrick and Lenski, 2009; Chubiz et al., 2012; Good et al., 2017; Lang et al., 2013; Traverse et al., 2013). At this point, the diversity and dynamics of the single-step beneficial mutations that constitute the clonal adaptome have typically been obscured by takeover of a few dominant mutants and further evolution of all lineages.

Several methods exist to characterize rarer mutations. Amplicon sequencing (e.g., as in FREQ-seq) is a straightforward strategy for profiling genetic variants in a targeted subset of a cell's genome (Chubiz et al., 2012; Fischer et al., 2017; Hong et al., 2018). However, the PCR enrichment step in this method requires optimizing conditions for each targeted region and introduces biases in inferring the frequencies of mutations that alter amplicon sizes. Another approach is to add unique molecular identifiers (UMIs) to the sequenced DNA fragments before any amplification steps. This information can be used to detect PCR duplicates to more accurately estimate mutation frequencies (Hong and Gresham, 2017; Kivioja et al., 2012) and to

correct sequencing errors (Schmitt et al., 2012). But, the extra depth of sequencing needed when using UMIs for error correction generally makes it infeasible to employ this approach on a genome-wide scale to track rare variants in many samples. Sequencing short barcodes inserted into the genomes of progenitor cells (BAR-seq) allows one to economically track the frequencies of extremely rare lineages derived from these cells (Levy et al., 2015; Venkataram et al., 2016); but, a limitation of this method is that the cell of interest must be genetically engineered with high efficiency to introduce a sufficient diversity of cellular barcodes, which may be difficult or impossible in certain cell types or clinical samples. Additional whole-genome sequencing is also required to identify the beneficial mutations that are linked to the winning barcodes.

Here, we describe multiplex adaptome capture sequencing (mAdCap-Seq). This method allows one to characterize many beneficial mutations in specific genes in a clonally evolving cell population. The key components of mAdCap-Seq are: (1) increasing sequencing depth in a targeted portion of a genome through hybridization-based DNA capture, (2) lowering sequencing error rates using UMIs, and (3) analyzing a time course of samples from a population during the early stages of clonal evolution. We tested mAdCap-Seq on laboratory populations that used the same ancestral strains and nearly identical culture conditions as a >70,000-generation *E. coli* evolution experiment (Lenski et al., 1991). We were able to directly identify diverse beneficial mutations in eight genes when they were orders of magnitude lower in frequency than could be accomplished by standard metagenomic sequencing. The molecular signatures and fitness effects of the many beneficial mutations found in three of these genes made it possible to infer the nature of selection acting on their functions in this environment. Our results demonstrate how mAdCap-Seq can be used to deeply profile a targeted portion of the adaptome of a cell.

RESULTS

Replaying the beginning of a long-term evolution experiment

We initially examined the evolution of nine replicate *E. coli* populations that were propagated via daily serial transfers in glucose-limited minimal medium for 500 generations. Our experiment used the same *E. coli* strains as the Lenski long-term evolution experiment (LTEE) and similar growth conditions (see **Methods**). Each population was inoculated with a 50/50 mixture of the two neutrally marked LTEE ancestor strains to visualize the initial selective sweep (Hegreness et al., 2006). An initial 30 generations of evolution occurred as these two strains were grown separately from single cells before they were combined to begin the serial transfers. Most populations maintained a roughly equal representation of descendants of both ancestral strains through the first 300 generations of the evolution experiment (**Fig. 1**). These dynamics are in agreement with what has previously been observed in studies of the LTEE, where few mutations reach a high frequency in the first few hundred generations of evolution (Good et al., 2017). We chose to further analyze only six of the nine populations due to constraints on how many samples we could process and sequence. Two *E. coli* populations (A4 and A5) were purposefully omitted because they exhibited early sweeps of one marker type, which indicates that their dynamics might have been dominated by one or a few "jackpot" mutations that occurred very early during outgrowth of these populations from single cells. The third population that was not selected for further study (A8) exhibited typical marker dynamics.

Tracking the trajectories of new beneficial mutations

We next performed mAdCap-Seq on eight genes at ~25 generation increments over the entire 500 generations of the evolution experiment for four of the six populations that we examined

142 further. These eight genes (*nadR*, *pykF*, *topA*, *spoT*, *fabR*, *ybaL*, *hslU*, and *iclR*) are known to be
143 targets of selection in the LTEE (Good et al., 2017; Tenaillon et al., 2016). Illumina libraries
144 containing UMIs (Schmitt et al., 2012) were prepared for sequencing and enriched for the
145 regions of interest using solution based hybridization (Bainbridge et al., 2010). Consensus
146 sequence reads were generated based on groups of reads with identical UMIs and aligned to the
147 *E. coli* genome to predict mutations, including using split-read mapping to identify transposon
148 insertions and large deletions (**Fig. 2A**). The enrichment procedure was effective: an average of
149 73.5% of consensus reads per sample mapped to the targeted regions that together constitute only
150 0.780% of the 4.63 Mbp genome. In the sample with the median number of total consensus
151 reads, the average coverage depth across each of the eight genes of interest exceeded 5,000 (**Fig.**
152 **2B**). After eliminating variants that exhibited systematic biases in their frequency trajectories
153 (see **Methods**), we were able to track the evolution and competition of 181 mutations, including
154 when many were present in less than 0.1% of the cells in a population (**Fig. 2C**, **Fig. 3**).
155 Mutation trajectories in all four populations exhibited a burst of genetic diversity in the
156 targeted genes followed by loss of this diversity. The initial dynamics are expected to be largely
157 driven by new genotypes that each evolve a single beneficial mutation very early in the
158 experiment. If their descendants escape stochastic loss, they will gradually increase in frequency
159 over the first few hundred generations as they outcompete the ancestral genotype. Once the
160 population becomes dominated by these first-step mutants, their frequency trajectories plateau
161 because of clonal interference: they are now mainly competing against one another and are
162 relatively evenly matched. In populations A1, A2, and A7, the total frequencies of the mutations
163 we identified sums to 49.6-62.4% at generation 297, indicating that each population is mostly

composed of genotypes with a mutation in one of the focal genes. We recovered less of the initial beneficial mutation diversity in population A3 where this sum was only 13.5%.

After around 300 generations, there is a steady decline in the frequencies of most mutations in the eight targeted genes. At this point, subpopulations of cells that have evolved multiple beneficial mutations begin to displace the genotypes that we initially tracked. Many of the most successful new genotypes are descended from cells that already had a mutation in one of the targeted genes. In these cases, the original mutations serve as markers for the further expansion of these subpopulations after a period during which their frequencies stagnate or decrease, but the new beneficial mutations responsible for this further increase in fitness are outside of the genomic regions we surveilled. The opposite situation, in which a beneficial mutation in one of the eight focal genes appears in a cell with an untracked beneficial mutation elsewhere in the genome, also occurs in a few cases. One example is a mutation in *pykF* that only appears after 300 generations in population A3 but then rapidly increases in frequency and becomes dominant. These dynamics indicate that its increase is accelerated by the presence of a prior, unknown beneficial mutation in the genetic background in which it evolved.

Fitness effects can be inferred from initial mutation trajectories

We next sought to calculate the fitness benefits of individual mutations by tracking how rapidly their frequencies rose early in the experiment when they were largely competing versus the ancestral genotype because all new mutations in the population were still rare. To that end, we performed mAdCap-Seq on all six populations at ~13-generation increments from 169 to 236 generations (**Fig. 2D**, **Fig. 3**). With this additional data we were able to track a total of 240 mutations as they gradually increased in frequency during the critical time window from

generation 163 to 243 that captures the dynamics of the first selective sweep. In the four populations we had already sequenced (A1, A2, A3, and A7), these mutations included 120 of the 181 previously found in the complete time course data spanning 500 generations and 54 additional mutations that had not been detected when analyzing the original time course data alone. Using the new mAdCap-Seq data, we also identified 66 mutations in the two populations for which we did not have time course data at 25 generation increments across the entire 500 generations of the evolution experiment (A6 and A9). Of the 240 total mutations, 93.3% occurred in just three of the eight targeted genes: *nadR*, *pykF*, and *topA* **(Fig. 4A)**.

We were able to estimate the fitness effect of each of these 240 beneficial mutations by fitting a binomial logistic model to how the counts of reads supporting the variant versus reference sequence increased over time from 163 to 243 generations. In all populations, there is initially a log-linear increase in the frequency of each mutation as the first wave of evolved cells, nearly all of which are expected to have just one of these beneficial mutations, competes against a population that is still almost entirely cells with the ancestral genotype. Then, there is a deceleration in the rate at which the frequencies of the new mutations increase around generation 196 that coincides with the onset of clonal interference. Genotypes with beneficial mutations begin to make up a sizable proportion of the population at this point, making it necessary to account for how they are increasingly competing against one another to estimate fitness effects.

We accounted for clonal interference by adding a stepwise increase in the average fitness of the entire cell population over time as an additional set of parameters to the binomial logistic model (**Fig. 2E**, **Fig. 3**). That is, we estimated how the fitness of the population, as a whole, was changing from the deceleration in the trajectories of the subset of mutations that we tracked in the targeted genes. Because overall population fitness dynamics are highly reproducible from

population to population in the LTEE conditions (Lenski et al., 1991), we used one consensus model of how the fitness of the populations increased (fit from all tracked mutations in all six sequenced populations) to correct our estimates of individual mutation fitness effects for clonal interference. Most of the increase in population fitness occurs rapidly in a single step during the interval spanning 196-209 generations. This rapid change followed by stasis may seem at odds with the continuing increase in the trajectories of many beneficial mutations. However, this type of stepwise increase is a typical result of clonal dynamics in models and experiments (Gerrish and Lenski, 1998; Lenski et al., 1991). It could result from many mutations with small fitness effects, no one of which reaches an observable frequency, peaking and then being outcompeted by the more highly beneficial mutations that we are able to track, for example.

The mean fitness effect that we inferred for the 240 tracked mutations in all six populations was 9.00% with a standard deviation of 1.33%. Although the distributions of the fitness effects estimated for mutations in *nadR*, *pykF*, and *topA* overlap **(Fig. 4B)**, there was a significant stratification among these genes. Mutations in *nadR* were 0.44% more beneficial than mutations in *topA*, on average, and this difference was significant ($p = 0.022$, one-tailed Mann–Whitney U test). In turn, mutations in *topA* were 0.70% more beneficial than those in *pykF* ($p = 0.00046$, one-tailed Mann–Whitney U test). The fitness effects of the 16 mutations in the other genes (*spoT*, *fabR, ybaL*, and *iclR*) were not significantly different from the those of the 224 mutations in *nadR*, *pykF*, and *topA* ($p = 0.33$, two-tailed Mann–Whitney U test). Thus, highly beneficial mutations are possible in these genes as well, but they occur at a much lower rate than similarly beneficial mutations in *nadR*, *pykF*, and *topA*.

One metric for how effectively we mapped the *E. coli* adaptome is the fraction of the increase in the fitness of each population that is captured by the subset of beneficial mutations

tracked with mAdCap-Seq. The fitness increase of each population could be reliably estimated by generation 196, and separate estimates for each population were in close agreement with the consensus estimate that included all populations after generation 209 (**Fig 1E**, **Fig. 2**). Thus, we could make robust calculations beginning at these time points. The percentage of the fitness increase contributed by the tracked mutations ranged from a low of 10.4% in population A9 to a high of 34.9% in population A2 at generation 223. The mean across all six populations was 27.5%. This fraction was not constant across time. As evolution continued, cells with these same mutations should account for a higher and higher fraction of the population fitness if they are displacing cells with less-beneficial mutations. In line with this expectation, they accounted for only 19.8% and 18.3%, on average, of the increase in population fitness earlier in the experiment, at generations 196 and 206, respectively. Later, the frequency trajectories plateaued for the beneficial mutations we tracked. This behavior means that the fitness of the whole population had caught up and was now roughly the same as the fitness of a cell with one of these beneficial mutations. Under this assumption, the tracked mutations account for 16.3–78.8% (42.9% on average) of the ~9% fitness increase observed at generation 270 in the four populations sequenced at this time. Overall, while we could account for a considerable portion of the fitness evolution of these populations with the mutations captured by mAdCap-Seq, mutations in other genes and/or less-beneficial mutations contributed more in most cases.

Beneficial mutations reveal different signatures of selection on gene function

Of the 301 total beneficial mutations that we were able to identify using mAdCap-Seq, 272 were in the *nadR*, *pykF*, or *topA* genes. This large set of beneficial mutations gave us the statistical power to test for several signatures of molecular evolution to ascertain what types of changes in

256 the function of each gene improved *E. coli* fitness in this environment. Each of the three genes
257 exhibited a distinct spectrum of beneficial mutations (**Fig. 5**). In some cases, different types of
258 mutations were also unevenly distributed throughout the sequences of these three commonly hit
259 genes and had noticeably different effects on bacterial fitness (**Fig. 6A**).

260 The *E. coli nadR* gene has three distinct functions related to NAD biosynthesis: (1) the N-
261 terminal domain is a helix-turn-helix that binds to DNA so that it can act as a negative
262 transcriptional regulator of NAD salvage and transport pathways; (2) the internal domain is an
263 NMN adenylyltransferase (Raffaelli et al., 1999); and (3) the C-terminal domain is predicted to
264 have ribosylnicotinamide kinase activity (Kurnasov et al., 2003). Large deletions, frameshifts
265 from small insertions or deletions (indels), insertions of transposable insertion sequence (IS)
266 elements, and base substitutions creating stop codons dominate the *nadR* mutational spectrum
267 (**Fig. 5**). These disruptive mutations, most of which are expected to result in complete loss of
268 gene function, are significantly overrepresented versus nonsynonymous base substitutions in the
269 first two domains of the gene compared to the remainder (13.7 odds ratio, $p = 1.2 \times 10^{-8}$, one-
270 tailed Fisher's exact test) (**Fig. 6A**). Yet, there was not a significantly greater fitness effect for
271 disruptive mutations compared to nonsynonymous mutations overall ($p = 0.063$, one-tailed
272 Mann–Whitney U test). These results indicate that complete inactivation of *nadR* yields the
273 maximum benefit possible for a mutation in this gene. Consistent with our observations from
274 mapping its adaptome, deletion of *nadR* has been shown to be highly beneficial in the very
275 similar environment of the LTEE (Barrick et al., 2009).

276 Pyruvate kinase 1 (*pykF*) catalyzes the final step of glycolysis, transferring a phosphate group
277 from phophoenolpyruvate (PEP) to ADP to generate pyruvate and ATP. It is a key enzyme in
278 regulating glycolytic flux (Kochanowski et al., 2013; Siddiquee et al., 2004). We observed an

intermediate representation of disruptive mutations in *pykF*: fewer than in *nadR* but more than in *topA* (**Fig. 5**). Nonsynonymous base substitutions in *pykF* tend to have a larger fitness effect than disruptive mutations ($p = 0.00031$, one-tailed Mann–Whitney U test) (**Fig. 6A**). This finding is in agreement with a study of various *pykF* alleles that arose in the LTEE which found that nearly all *pykF* point mutations were more beneficial than deletion of the *pykF* gene, both in the ancestor and in evolved genetic backgrounds (Peng et al., 2018). PykF forms a homotetramer in which each polypeptide folds into three structural domains (Donovan et al., 2016; Mattevi et al., 1995). The central domain A forms the active site at the interface with domain B and the binding site for the allosteric effector fructose 1,6-bisphosphate at the interface with domain C. The nonsynonymous mutations that we observed are more concentrated than expected in domain A versus the other structural domains based on their relative lengths in the gene sequence ($p = 0.0018$ one-tailed binomial test) (**Fig. 6B**). Overall, adaptome mapping finds that complete inactivation of *pykF* is highly beneficial in the environment of our evolution experiment, but mutations that alter its activity—likely in ways that reduce glycolytic flux—are even more so. These results are consistent with a hypothesis that reducing *pykF* activity is beneficial in the similar glucose-limited conditions of the LTEE because this allows more PEP to be diverted to power import of glucose into cells via the phosphotransfer system (Woods et al., 2006).

DNA topoisomerase I (*topA*) relaxes negative supercoiling introduced into the chromosome by replication and transcription (Massé and Drolet, 1999). The mutations we observed in *topA* are almost exclusively single-base substitutions (**Fig. 5**). This type of adaptome signature implies that modulating the enzymatic activity of TopA provides the greatest fitness benefit. Complete loss of *topA* gene function is lethal to *E. coli* without compensatory mutations in DNA gyrase (Dinardo et al., 1982; Pruss et al., 1982). The structure of *E. coli* TopA consists of four N-

302 terminal domains (D1-D4) that make up the catalytic core and five C-terminal zinc finger and
303 ribbon domains (D5-D9) (Tan et al., 2015). The few out-of-frame indels and the large deletion
304 that we observe truncate TopA within domains D7-D9, which interact with single-stranded DNA
305 and with RNA polymerase but are not critical for catalysis. Considering only the catalytic core,
306 we find that nonsynonymous mutations are more concentrated in domains D1 and D4 versus D2
307 and D3 than expected from their relative sizes (p = 0.00068, one-tailed binomial test) (**Fig. 6C**).
308 D1 and D4 together form the ssDNA binding groove leading to the active site, and D1 also forms
309 part of the active site at its interface with D3 (Perry and Mondragón, 2003). Several base
310 substitutions in *topA* have been shown to increase positive supercoiling in evolved LTEE strains
311 (Crozat et al., 2005, 2010). The exact reason that this change in supercoiling is beneficial is
312 unknown, but it may be linked to increasing the expression of ribosomal RNAs (Crozat et al.,
313 2005), altering gene regulation responses to starvation or other stresses (Crozat et al., 2010),
314 and/or increasing the expression of genes in divergently transcribed operons (Houdaigui et al.,
315 2019).
316
317 **Recurrent beneficial mutations do not have greater fitness effects**
318 We observed many examples of exact genetic parallelism. That is, the same mutation occurred
319 and reached high frequency in different experimental populations. Each of these *E. coli*
320 populations was founded from single cells, so we can conclude that these recurrent genetic
321 changes are due to independent mutational events. We observed a total of 252 distinct genetic
322 changes across all eight profiled genes and 31 of these were found in more than one population.
323 While no single genetic change was detected in all six populations, 2, 2, 8 and 19 changes were
324 detected in 5, 4, 3, and 2 populations, respectively. Most of these were in the three genes that

were the main targets of selection (*nadR*, *pykF*, and *topA*), but one that occurred in three populations was in *fabR*. These mutations may be recurrent because they have a higher fitness benefit than other mutations, occur at a higher rate than other mutations, are more easily detected in the sequencing data, or due to some combination of these factors. We had fitness effect estimates for all of the 31 recurrent mutations and for 167 mutations that were each observed in only one population. The recurrent mutations had a 0.12% greater fitness effect, on average, compared to the singleton mutations, but this difference was not significant ($p = 0.25$, one-tailed Mann–Whitney U test). Thus, it is unlikely that many cases of exact genetic parallelism are due to these mutations being more beneficial than others in our dataset.

DISCUSSION

We used mAdCap-Seq to profile bacterial evolution during the initial stages of clonal competition when there is a burst of beneficial genetic diversity as many new subpopulations with different mutations evolve and begin to displace the ancestral genotype. We focused on eight genes known to accumulate adaptive mutations in the >70,000 generation Lenski long-term evolution experiment (LTEE) with *E. coli* that used nearly the same environment as our experiments. The only difference was that we added four times as much of the limiting nutrient (glucose). By combining Illumina sequencing using UMIs for error correction, hybridization-based capture of DNA encoding these genes, and dense temporal sampling, we were able to identify more beneficial mutations and track them at much lower frequencies than is possible with standard metagenomic sequencing. We detected a total of 301 mutations in the focal genes: 181 in the complete time courses of four populations and 240 during the initial selective sweep in these populations and two others, with 120 mutations overlapping between the two sets.

By densely sampling and deeply sequencing *E. coli* populations, we were able to characterize many beneficial mutations that never reached the normal detection limit of Illumina sequencing before they become casualties of clonal interference. Only 13 of the 181 mutations we detected in the complete time courses ever achieved a frequency of 5% or more, which can be reliably distinguished from noise without the use of UMIs or other error correction techniques, and only seven were this common for 100 or more generations, such that they were likely to be detected by a typical time-sampling scheme. Considering all of our data sets, we characterized 241 and 42 mutations that never reached 1% or 0.1% thresholds, respectively, at any sampled time point. Our success in recovering rare variants meant that we discovered more examples of beneficial mutations in the three commonly mutated genes (*topA*, *pykF*, and *nadR*) than have been reported in all prior studies of the evolution of the twelve LTEE populations through 60,000 generations of evolution (Barrick et al., 2009; Deatherage et al., 2015; Good et al., 2017; Ostrowski et al., 2008; Tenaillon et al., 2016; Woods et al., 2006). These large sets of mutations enabled us to identify distinct molecular signatures of adaptation in each protein.

mAdCap-Seq profiles genetic variation in specific genes. Whether and to what extent mutations in a given gene contribute to a cell's adaptome depends on a combination of two main factors: how many mutations in that gene are sufficiently beneficial that they can compete with other top mutations (the distribution of fitness effects) and the chances that these mutations will evolve (the mutational target size). For the three genes with the most mutations in our experiment, we can rationalize the rank-order of their representation (*nadR* > *pykF* > *topA*) in terms of these parameters. First, mutations that we tracked in *nadR* are more beneficial than mutations in the other two genes, on average. Because complete loss of function of this gene is maximally beneficial, the target size for these mutations is also larger, as it includes not only

base substitutions but also small indels causing frameshifts, larger deletions, and IS element insertions. The next most commonly mutated gene is *pykF*. The mutations we identified in *pykF* are actually slightly less beneficial on average than the mutations in *topA*. However, mutations that completely knock out *topA* function are not represented in the adaptome, whereas these types of mutations in *pykF* are highly beneficial. In this case, larger target size appears to outweigh smaller fitness effects in determining the representation of mutations in each gene.

From our experiment alone, it is unclear why mutations in the other five captured genes are rarer in the adaptome. We detected no mutations in *hslU* and *iclR*. Mutations we tracked in the other three genes (*spoT*, *fabR*, and *ybaL*) do not have significantly different fitness effects from those in the three genes with the most mutations (*nadR*, *pykF*, *topA*). However, our statistical power for detecting differences is limited by the small number of mutations detected in these genes, so we cannot definitively conclude that they are underrepresented solely due to having smaller target sizes for top-flight mutations. As described below, comparing our results to the long history of the LTEE does provide some further insights into why mutations in each of the genes that we profiled are more or less abundant in the adaptome in our evolution experiment.

We captured beneficial mutations in eight genes known to be targets of selection in the LTEE. Mutations in four of these (*topA*, *pykF*, *spoT*, and *fabR*) reach high frequencies within the first 1,000 generations of the LTEE in multiple populations (Deatherage et al., 2015; Good et al., 2017). Mutations in the other four (*hslU*, *nadR*, *ybaL*, and *iclR*) are also common in the LTEE, but they typically occur later (often within the first 2,000 to 10,000 generations) (Good et al., 2017; Tenaillon et al., 2016). Nearly all mutations in these genes in our evolution experiment were in *topA*, *pykF*, and *nadR*, but we also found multiple mutations that were similarly beneficial in *spoT*, *fabR*, and *ybaL*. Mutations in *nadR* were more widespread than expected in

394 our experiment and may be more likely to completely disrupt its function than beneficial alleles
395 that evolve in the LTEE (Ostrowski et al., 2008). Mutations in *spoT* and *fabR* were rarer than
396 expected from the LTEE. The increased concentration of glucose in our experiment compared to
397 the LTEE may explain these slight differences. These results are reminiscent of how changing a
398 different aspect of the LTEE environment (temperature) re-focused the mutations of largest
399 benefit that succeeded early onto different genes in two prior studies (Deatherage et al., 2017;
400 Tenaillon et al., 2012). Despite the subtle difference between the LTEE and our experiment, we
401 were still able to use mAdCap-Seq to effectively map the adaptome. We accounted for the
402 majority of the genetic variation present after the first sweep in three of the four populations that
403 we profiled over the entire 500 generations by capturing mutations in just eight genes.
404 We can ask to what extent profiling mutations while they were rare by mAdCap-Seq gave
405 'early warning' of mutations driving adaptation in these clonal cell populations. In general, we
406 were able to begin tracking most mutations when they were above a frequency of 0.01%. This
407 level of profiling enabled us to first detect mutations an average of 69, 150, and 290 generations
408 before they surpassed frequencies of 0.1%, 1%, and 5%, respectively. Under the conditions of
409 our experiment these intervals take roughly 10, 23, and 44 days, respectively. (The amount of
410 lead time becomes disproportionately longer when requiring a mutation to reach higher
411 frequencies due to clonal interference between beneficial mutations.) Therefore, even though we
412 made these observations retrospectively, there would have been sufficient time to complete the
413 DNA isolation, library preparation, sequencing, and analysis steps in mAdCap-Seq quickly
414 enough for this approach to give early warning of the types and targets of genetic variants
415 driving evolution of these populations. The chances and timescales of early detection would be
416 expected to increase even more if ecological interactions or spatial structure further slowed the

takeover of new variants, as has been demonstrated and discussed in other microbial evolution experiments (Baym et al., 2016; Frenkel et al., 2015; Traverse et al., 2013).

Genes in which we observe early, but unsuccessful beneficial mutations may acquire mutations again and again until they are successful in a population's evolutionary future. The extent to which this occurs is determined by the nature of epistatic interactions. In the LTEE and other microbial evolution experiments, diminishing returns epistasis dominates between beneficial mutations in different genes (Chou et al., 2011; Khan et al., 2011; Kryazhimskiy et al., 2014; Wei and Zhang, 2019; Wiser et al., 2013). That is, mutations in one gene that improve the fitness of the ancestor tend to still be beneficial to evolved genotypes containing beneficial mutations in other genes, just less so than when those other mutations are present. Subpopulations with mutations in both *nadR* and *pykF* evolve by 20,000 generations in all 12 LTEE populations, and cells that also contain a mutation in *topA* are found in six of the LTEE populations at this point (Tenaillon et al., 2016). By this time, mutations in *ybaL* and *spoT* are also found in nine and six LTEE populations, respectively. So, for five of the six genes in which we detected multiple mutations in the initial burst phase, it is likely that nearly all of them would have eventually accumulated beneficial mutations if we continued our experiment.

The other three genes (*fabR*, *iclR*, and *hslU*) likely represent other scenarios. Mutations in *fabR* transiently appear within the first 2,000 generations of the LTEE (Deatherage et al., 2015). They interact unfavorably with beneficial mutations in *spoT* and other genes, such that a *fabR* mutation essentially precludes further adaptation by mutating the other set of genes and vice-versa (Deatherage et al., 2015; Woods et al., 2011). We detected 9 mutations in *fabR*, which was more than the five we observed in *ybaL*. However, we predict that *fabR* mutations are unlikely to re-emerge and be successful in the future of these populations because of their negative

interactions with other beneficial mutations. On the other hand, we detected only a single mutation in *iclR* and a single mutation in *hslU*. Of the 12 LTEE populations, 11 have sizable subpopulations with mutations in *iclR* and 11 have mutations in *hslU* by 20,000 generations, which makes them more common than mutations in *spoT* and *ybaL* in the long run. Therefore, mutations in *iclR* and *hslU* appear to either require the presence of mutations in other genes to become highly beneficial or may not be able to experience any mutations that are beneficial enough to make them competitive early on in our experiment.

The nature of epistasis and the limits that it imposes on predicting the future evolution of a cell population could be further probed using mAdCap-Seq in several ways. One could repeat the evolution experiment beginning with genotypes containing different first-step beneficial mutations and compare their adaptomes. One could also interrogate the diverse collections of cells containing different beneficial alleles that we have evolved, by taking the 150-generation populations and further evolving them under different conditions to map genotype by environment effects, for example. Such experiments might also reveal latent beneficial mutations in other genes (e.g., *iclR* and *hslU*) that were able to outcompete the ancestor in our experiment but remained below the detection limit because they were not as beneficial as mutations in *topA*, *pykF*, and *nadR* in this environment. There is precedent for changes in the environment reorienting selection to different subsets of the same genes. In an offshoot of the LTEE that began with a clone that had *spoT*, *topA*, and *pykF* mutations, selection focused further mutations on either *hslU*, *iclR*, or *nadR* depending on changes in temperature (Deatherage et al., 2017).

mAdCap-Seq is one among several high-throughput methods for interrogating the possibilities that a cell's descendants can explore in its fitness landscape. Different approaches reveal complementary types of information and have different limitations. For example, deep

mutational scanning uses high-throughput sequencing to simultaneously query large libraries of mutations in a single gene (Fowler and Fields, 2014). Transposon insertion sequencing (Tn-Seq) allows one to infer the fitness effects of transposon insertions in essentially every gene in a genome (van Opijnen and Camilli, 2013). While nearly all Tn-Seq mutations disrupt gene function, CRISPR-enabled trackable genome engineering can make genetic changes of other types, including those that increase expression of a target gene, and track the abundance and thereby fitness of these variants in parallel by sequencing barcodes (Garst et al., 2017). These and other related methods rely on artificially constructing variant libraries and may test mutations in a nonnatural context (e.g., in genes on a plasmid). Thus, they do not provide information about which genetic variants are accessible by spontaneous mutations.

Methods that characterize just those mutations that spontaneously arise in clonally evolving cell populations more specifically map adaptomes. For example, a capture-based enrichment and high-throughput sequencing method, similar to mAdCap-Seq but without UMIs, has been used to detect rare mutations in circulating tumor DNA in patient blood samples (Newman et al., 2014, 2016). FREQ-Seq is an example of a multiplexed amplicon sequencing approach that is similar to mAdCap-Seq in how it aims to track the frequencies of new beneficial mutations in specific, targeted regions of microbial genomes (Chubiz et al., 2012). When not employing UMIs for error correction, amplicon sequencing has a limited ability to differentiate extremely rare mutations from sequencing errors (Schmitt et al., 2012). Another issue is that the initial PCR steps used to create amplicons can bias detection. In our experiment with *E. coli*, IS element insertions are common. DNA templates with such large insertions would be highly disfavored during PCR amplification, leading one to greatly underestimate the frequencies of these mutations. By contrast, the hybridization-based capture approach utilized by mAdCap-Seq

for target enrichment recovers DNA fragments with these and other types of mutations with the same efficiency. Large deletions in an evolved genome that completely remove a targeted region are an exception. These mutations create a blind spot for both amplicon and capture enrichment approaches. The lack of any reads from genomes with the deletion will lead to overestimating the frequencies of other mutations that preserve recovery of DNA from the region. While this is a general caveat that should be considered when using these approaches, large deletions are unlikely to have affected our mAdCap-Seq results. The genes we captured are rarely mutated in this way in the LTEE, and we tracked mutations early in the evolution of these populations from single cells when all new genetic variants were still rare.

BAR-seq represents a class of lineage-tracking methods that can be used to characterize spontaneous mutations through monitoring changes in the frequencies of barcode sequences inserted into the genomes of cells (Blundell and Levy, 2014). Since all high-throughput sequencing reads can be concentrated into counting barcodes that differ from one another (to the extent that sequencing errors do not affect proper assignment), these methods can track rarer subpopulations of cells than mAdCap-Seq. This means they can characterize essentially all of the beneficial mutations competing in a population. For comparison, we tracked ~60 mutations per *E. coli* population in the initial selective sweep, but tens of thousands of mutations have been analyzed in this way using BAR-seq on a single yeast population (Levy et al., 2015). Thus, lineage-tracking methods have much greater power for reconstructing the distribution of fitness effects of all mutations that spontaneously arise in a cell population. However, there are trade-offs relative to other approaches. Additional post-hoc whole-genome sequencing of many isolates from the evolved population is needed to link each barcode to a mutation causing the observed fitness change (Venkataram et al., 2016). But the foremost consideration is that one

must genetically engineer cells to introduce barcodes into their genomes. This limitation has restricted the use of BAR-seq to populations of model organisms evolved in the laboratory so far.

The adaptome is the neighborhood of accessible genetic changes that are most likely to become dominant and contribute to ongoing adaptation of a population. We have demonstrated how mAdCap-Seq can be used to deeply profile a targeted portion of the adaptome of a bacterial cell undergoing clonal evolution in a controlled laboratory environment. Mapping clonal adaptomes, which consist solely of *de novo* beneficial mutations, is likely to be of particular interest and utility in systems that evolve repeatedly from a defined starting point. These range from bioreactors that are seeded with the same engineered strain in different production runs to lung infections in cystic fibrosis patients that start from similar, but not identical, strains of opportunistic pathogens. This approach could also be used to probe the fitness landscapes underlying how human infections and cancers evolve drug resistance and greater pathogenicity. Mapping out the likely evolutionary possibilities in these systems can potentially allow one to monitor for the appearance of especially costly or dangerous mutations and could even lead to developing interventions that deflect the population from these undesirable adaptive pathways.

Outside of the laboratory, some of the simplifying assumptions used in our study break down. In may be difficult or impossible to sample a new cell population found in the environment or in a patient multiple times during the critical time window before it has already evolved substantial genetic diversity. Furthermore, many microbes have mechanisms for sexual recombination that can rapidly combine multiple beneficial mutations into one genome, which may violate our assumption that double mutants are rare during the first selective sweep. While these real-world situations complicate evaluating the relative benefits of each new genetic variant

from sequencing alone, mAdCap-Seq would still be a useful approach for characterizing whether mutations in specific genes are contributing to the leading edge of adaptation in these situations.

ACKNOWLEDGEMENTS

The authors acknowledge several anonymous reviewers for helpful feedback and the Texas Advanced Computing Center (TACC) at The University of Texas at Austin for providing high-performance computing resources. Funding: this work was supported by the Cancer Prevention & Research Institute of Texas (CPRIT) (RP130124), the National Institutes of Health (R00GM087550 and R01GM088344), the National Science Foundation (CBET-1554179 and DEB-1813069), and the NSF BEACON Center for the Study of Evolution in Action (DBI-0939454). D.E.D. acknowledges support from a University of Texas at Austin CPRIT research traineeship (RP101501). The funders had no role in study design, data collection and analysis, decision to publish, or preparation of the manuscript.

AUTHOR CONTRIBUTIONS

Conceptualization, data curation, funding acquisition, methodology, software, visualization, writing – original draft, writing – review & editing: D.E.D. and J.E.B; Investigation: D.E.D; Supervision: J.E.B.

DECLARATION OF INTERESTS

J.E.B. is the owner of Evolvomics LLC. D.E.D. has been a paid consultant for Evolvomics LLC.

FIGURES

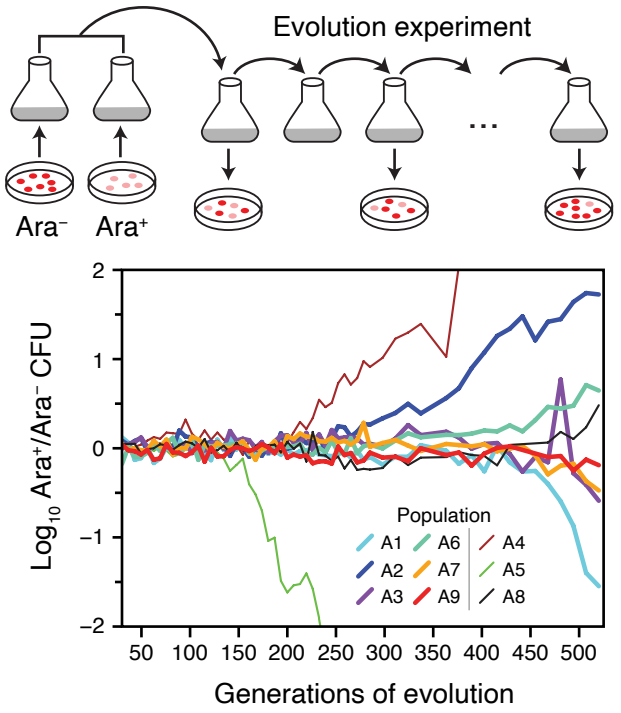

Figure 1. Replaying the first selective sweep of a long-term evolution experiment. Nine *E. coli* populations were initiated from equal mixtures of two variants of the ancestral strain that differ in a neutral genetic marker for arabinose utilization (Ara). We observed the evolutionary dynamics of these populations over 500 generations of regrowth from 75 daily 1:100 serial transfers by periodically plating dilutions of each population on indicator agar. Each ancestral strain subpopulation was derived from a single colony isolate that experienced 30 generations of growth before it was combined with the opposite type to initiate the serial transfers. The ratio of Ara^+ cells (pink colonies) to Ara^- cells (red colonies) diverges from 1:1 when descendants of one ancestor type accumulate enough of a fitness advantage due to *de novo* beneficial mutations that they take over. We focused further analysis on six of the nine populations (thick lines).

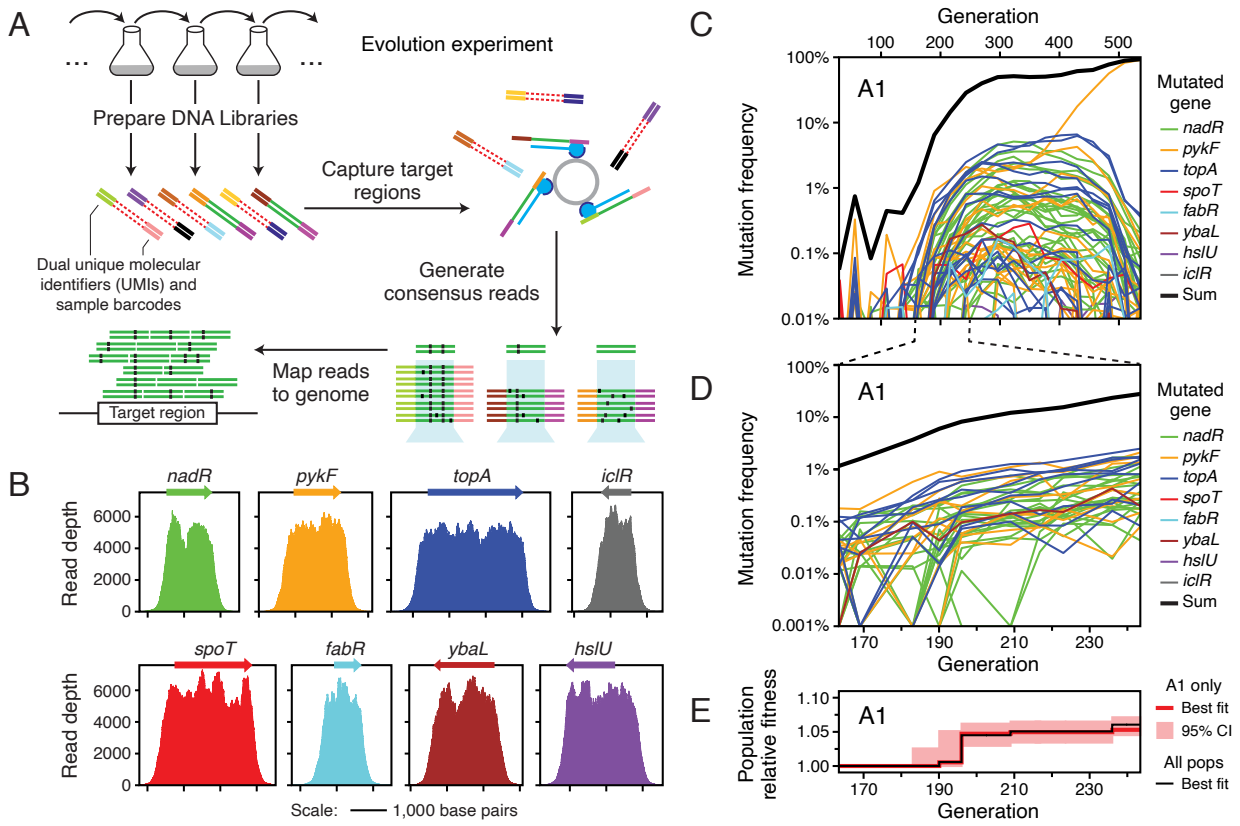

Figure 2. Profiling many beneficial mutations in the first selective sweep by deep sequencing. (A) Schematic of the deep sequencing approach. Genomic DNA is directly isolated from the *E. coli* populations and prepared for paired-end Illumina sequencing with sample barcodes and dual UMIs (colored ends attached to red/green double stranded DNA). DNA fragments matching the targeted genome regions (green centers) are captured by probes (blue) bound to magnetic beads and other sequences are washed away (red centers). Reads in pairs that have the same dual unique molecular identifiers, which implies that they were PCR amplified during library preparation from the same original genomic DNA fragment, are used to construct consensus reads to eliminate sequencing errors. Consensus reads are mapped to the reference genome to call sequence variants. (B) Enrichment of reads mapping to eight genes known to be early targets of selection in this environment from the long-term evolution experiment. The final coverage depth of consensus reads in and around these genes is shown for a typical sample

(population A7 at 500 generations). (C) Frequency trajectories for mutations in the eight targeted genes as well as the sum total frequency in population A1 over the complete time course of the evolution experiment. When a mutation was not detected at a time point, its trajectory is shown as passing through a frequency of 0.0001% (outside of the plot bounds). (D) Mutation frequency trajectories for population A1 during the selective sweep window from 163 to 243 generations when mutations were first reaching detectable frequencies and outcompeting the ancestral genotype. At time points when a mutation was not detected, its frequency is shown as 0.001% (at the bottom of the plot). (E) Estimated relative fitness of population A1 in each interval between sequenced time points. The frequency trajectories of all beneficial mutations in the initial sweep shown in D were used to jointly estimate the average fitness of the entire population from the deceleration in the rate of increase of the observed mutation trajectories as genotypes with beneficial mutations became common (see **Methods**). This fitness trajectory fit accounts for all cells in the population, regardless of whether they have a mutation in the targeted genes or elsewhere in the genome. The red line is the maximum likelihood estimate of the population fitness trajectory. The red shading around it shows 95% confidence intervals on this value in each interval. The black line shows the increase in fitness estimated for a consensus model that was jointly fit to all mutations tracked in all six populations. The consensus population fitness trajectory was used when estimating the fitness effects of individual mutations (see **Methods**).

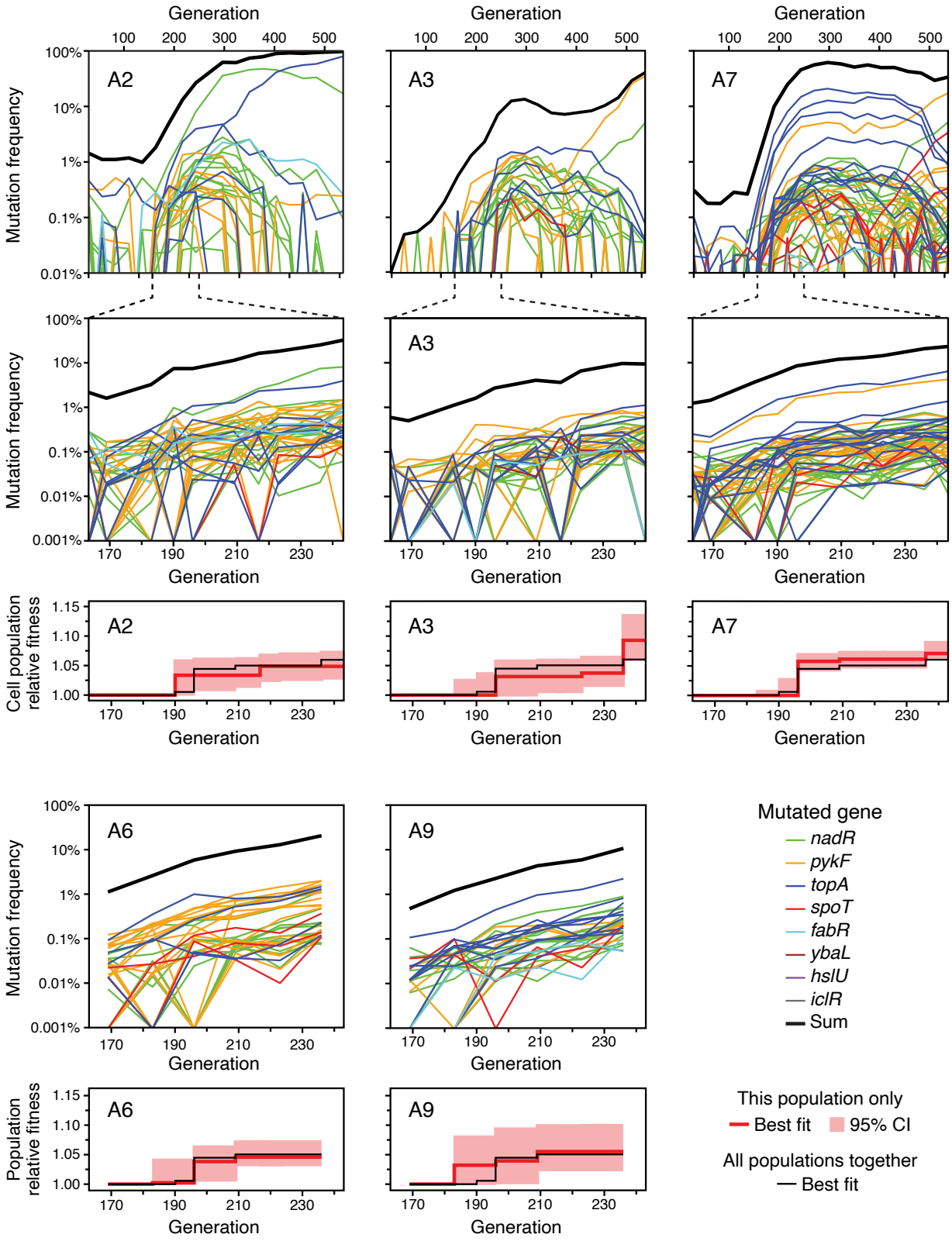
Generation
100
200
300
400
500
A2
A3
A7
Mutation frequency
100%
10%
1%
0.1%
0.01%
0.001%
170
190
210
230
A6
A9
Cell population relative fitness
Population relative fitness
1.15
1.10
1.05
1.00
Mutated gene
nadR
pykF
topA
spoT
fabR
ybaL
hslU
iclR
Sum
This population only
Best fit
95% CI
All populations together
Best fit

597

598

Figure 3. Frequency trajectories of mutations in the remaining populations. The same plots described in Figure 2C-E for population A1 are shown for populations A2, A3, and A7 (top three sets of panels). For populations A6 and A9, sequencing was only performed at time points during the selective sweep window from 169 to 236 generations so only the plots corresponding to Figure 2D-E are shown (bottom two sets of panels).

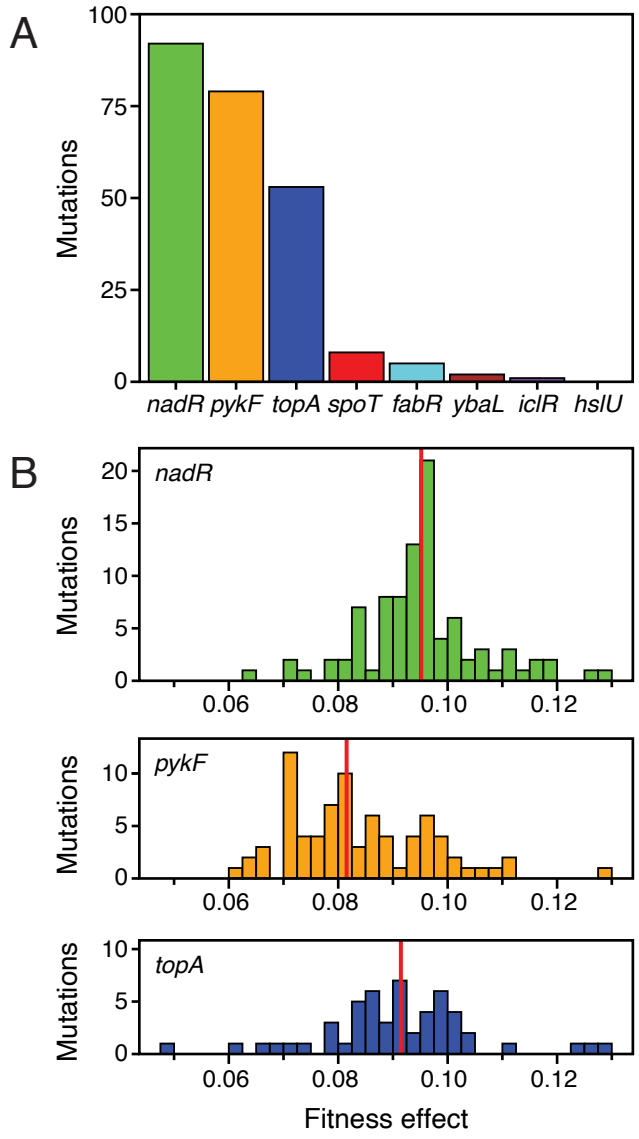

Figure 4. Characteristics of beneficial mutations in the initial selective sweep. (A) Total number of beneficial mutations in each of the eight targeted genes for which fitness effects could be estimated by analyzing their frequency trajectories between generations 163 and 243. (B) Distributions of fitness effects of beneficial mutations in the three genes that were the dominant targets of selection. Mutations are binned by the maximum likelihood estimates of their fitness effects. Vertical red lines show the mean of each distribution. 95% confidence limits in **Figure 6A** show uncertainty in the fitness effect estimated for each of these mutations.

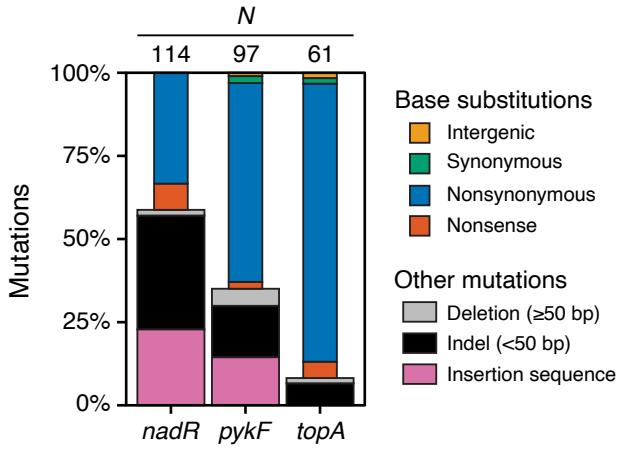

612

613 **Figure 5. Spectra of early beneficial mutations in *nadR*, *pykF*, and *topA*.** These three genes
614 were the dominant targets of selection during the evolution experiment among the eight genes
615 profiled for beneficial mutations. The total number of mutations identified in each gene is
616 indicated above its column. The width of the bars distinguishes base substitutions (thin bars)
617 from other types of mutations (thick bars).

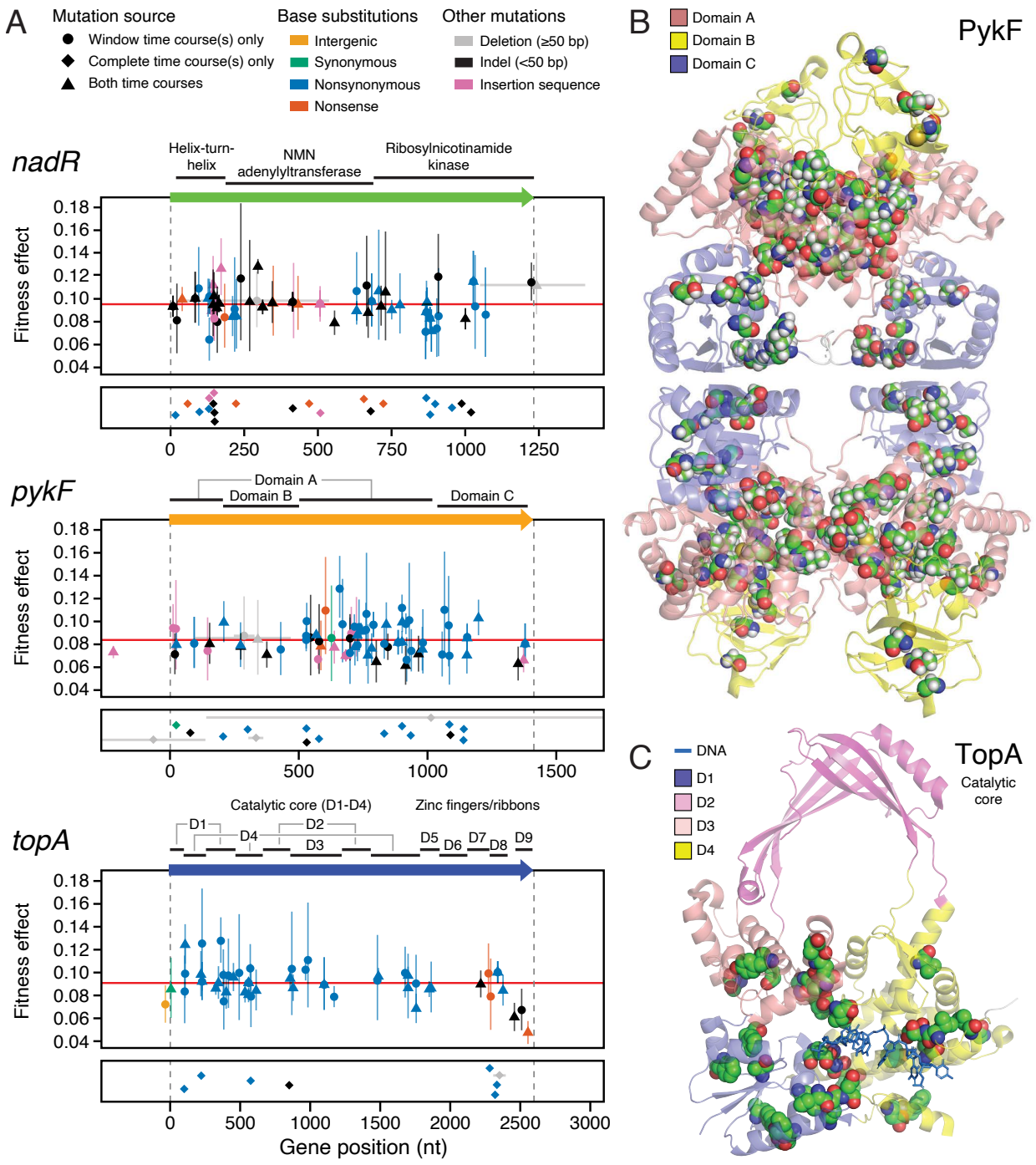

Figure 6. Mutations in the three genes that were the dominant targets of selection. (A) Nucleotide positions and properties of all mutations found in each of the three genes that were the dominant targets of selection during the evolution experiment. Colors represent the type of mutation. Symbols indicate whether each mutation was detected in the selective sweep window,

623 the complete time course, or both. The upper panel for each gene, shows the fitness effects
624 estimated for mutations in that gene. Error bars are 95% confidence limits. When the same
625 genetic change was detected in multiple populations, information from all of its frequency
626 trajectories was combined to estimate one overall fitness value and confidence limit for all of
627 those mutations (see **Methods**). Thus, the symbols and error bars completely overlap for each
628 independent occurrence of these mutations in a different population. The reading frame of the
629 gene is shown above this panel with protein domains labeled. Vertical dashed grey lines
630 represent the start and end of each gene. Horizontal grey lines show the extent of large deletions
631 within the pictured region. Horizontal red lines represent the average fitness effects for all
632 mutations in a gene. The lower panel for each gene shows mutations that were only detected in
633 the complete time courses and therefore do not have an estimated fitness effect. Symbols in this
634 panel are randomly jittered in the vertical direction to improve their visibility. (B) Structural
635 context of mutations in PykF. Sites of nonsymonymous mutations are highlighted by showing
636 space-filling models of the ancestral amino acid residues. All four subunits of the PykF
637 homotetramer are shown. (C) Structural context of mutations in the catalytic core of TopA. Sites
638 of nonsymonymous mutations are highlighted by showing space-filling models of the ancestral
639 amino acid residues. Only domains D1-D4 are present in the structure. The DNA strand
640 interacting with TopA is shown as a stick model.

STAR★METHODS

Resource Availability

Lead Contact

Lead contact, Jeffrey E. Barrick (jbarrick@cm.utexas.edu), will provide additional information and fulfill any requests for materials.

Materials availability

Frozen *E. coli* populations from each sequenced time point are available.

Data and code availability

Illumina sequencing reads associated with this study have been deposited into the NCBI Sequence Read Archive (Accession: PRJNA601748). Code used for analysis and figure generation is archived on Zenodo (DOI: 10.5281/zenodo.5092871).

Experimental Model and Subject Details

Bacterial Strains and Culture Conditions

E. coli B strains REL606 and REL607 and growth conditions are derived from the Lenski long-term evolution experiment (Lenski and Travisano, 1994; Lenski et al., 1991). REL606 and REL607 differ by a mutation in an arabinose utilization gene enabling us to monitor their relative frequencies during the evolution experiment (Lenski et al., 1991). Growth was carried out in 50 mL Erlenmeyer flasks in 10 mL of Davis Minimal (DM) media supplemented with 100 mg/L glucose (DM100). DM is made by dissolving 5.3 g/L K_2HPO_4, 2 g/L KH_2PO_4, 1 g/L $(NH_4)_2$ SO_4, and 500 mg/L $Na_3C_6H_5O_7$ $(H_2O)_2$ in water. After autoclaving, 1 mL/L of a 10% (w/v) $MgSO_4$ stock solution (separately autoclaved) and 1 mL/L of a 0.2% (w/v) stock solution of thiamine (filter sterilized) are added. DM100 has a slightly higher concentration of glucose than the 25

mg/L glucose (DM25) used in the LTEE, but it still well below the ~1000 mg/L concentration at which nutrients other than glucose begin to limit growth in this medium. We used this higher glucose concentration to ensure we had enough cells for sequencing and archiving. Liquid cultures were grown at 37°C with orbital shaking over a one-inch diameter at 120 RPM.

Method Details

Evolution experiment

Nine colonies of *E. coli* B strain REL606 and nine of strain REL607 were selected at random and used to inoculate separate flasks containing 10 mL of DM25. Approximately 30 generations of growth occurred starting from the initial single cell that gave rise to each colony until saturation of these cultures. Populations A1 through A9 were founded by inoculating 10 mL of fresh DM100 with 50 µL of one REL606 culture and 50 µL of one REL607 culture. The remaining culture volume for all 18 founding colonies was archived in 15 mL conical tubes at −80°C with 2 mL dimethyl sulfoxide (DMSO) added as cryoprotectant. Every 24 hours, 100 µL of overnight culture was transferred to 10 mL of fresh DM100, and the remaining culture volume was archived in the same way. This procedure was continued through 75 daily transfers. Periodically 1 µL of culture was diluted 10,000-fold in sterile saline and plated on tetrazolium arabinose (TA) agar to allow growth of ~200 colonies. TA agar is made by adding 10 g/L tryptone, 1 g/L yeast extract, 5 g/L NaCl, and 16 g/L agar to water and autoclaving. Then, a separately autoclaved solution of 10 g/L arabinose in water is added. The combined volume of these two solutions is such that it yields the indicated final concentrations of each component. Roughly 4/5 and 1/5 of the total volume are used for the two solutions, respectively. As the solution cools, 1 mL/L of 5% (w/v) triphenyl tetrazolium chloride (filter sterilized) is added. On TA plates, the mutation in the

arabinose utilization gene makes REL606 (Ara^-) colonies red and REL607 (Ara^+) colonies pink (Lenski et al., 1991). The ratio of red to pink colonies was used to monitor these populations for selective sweeps (Hegreness and Kishony, 2007; Woods et al., 2011).

DNA isolation and library preparation

Genomic DNA (gDNA) was isolated from frozen population samples by first thawing each 15 mL conical tube on ice. Of the ~12 mL total volume of culture plus cryoprotectant, 1.2 mL was transferred to a 2 mL cryovial and refrozen. The remaining ~10.8 mL was centrifuged at 6,500 × g at 4°C for 15 minutes. The resulting cell pellets were transferred with a volume of remaining solution to 1.7 mL Eppendorf tubes. Then, gDNA was isolated using the PureLink Genomic DNA Mini kit (Life Technologies). For each sample, 1 µg of gDNA was randomly fragmented on a Covaris S2 Focused Ultrasonicator.

Illumina libraries were constructed using the Kappa Biosystems LTP Library Preparation Kit with the following modifications. Following the end-repair step, fragmented DNA was T-tailed (rather than A-tailed) in a 50 µl reaction including 10 mM dTTP and 5 units of Klenow fragment, exo^- (New England Biolabs). In the adapter ligation step, modified Illumina adapters containing 12-base unique molecular identifiers were ligated to the T-tailed fragments as previously described (Schmitt et al., 2012). Adapters used here differ slightly from those used in (Schmitt et al., 2012) as full-length adapter sequences containing unique external sample barcodes were directly ligated to the T-tailed dsDNA inserts to reduce the risk of cross-contamination between samples. The full list of DNA sequence adaptors is provided in **Table S1**.

Probe design and target capture

Oligonucleotide probes consisting of 60-base xGen Lockdown probes (Integrated DNA Technologies) were designed to tile across each of the eight genes of interest including upstream promoter elements. Probes for each gene were compared to the entire *E. coli* B strain REL606 reference genome (GenBank: NC_012967.1) (Jeong et al., 2009) using BLASTN (Camacho et al., 2009). The starting positions of all probes in a set were shifted by one base at a time until every probe had only a single significant predicted binding location (match with E-value < 2×10^{-5}). The sequences of the final set of 242 probes are provided in **Table S2**.

Capture was performed using a SeqCap EZ Hybridization and Wash Kit (NimbleGen). The procedure in the SeqCap EZ Library SR User Guide v3.0 (NimbleGen) was followed with several modifications. First, 18 to 20 population samples with different sample barcodes were pooled together in a single capture reaction that contained a total of 1 μg of library DNA from all samples, 1 mmol of a universal blocking oligo, and 1 mmol of a degenerate sample barcode blocking oligo. The sequences of these blocking oligos are provided in **Table S3**. Second, after hybridization for 72 h, DNA fragments hybridized to the biotinylated probes were recovered using MyOne Streptavidin C1 Dynabeads (Life Technologies). Third, a final 8-cycle PCR step was performed with HiFi Hotstart DNA Polymerase (Kappa Biosystems).

Sequencing

Paired-end 101- or 125-base sequencing of the final libraries was performed on an Illumina HiSeq 2000 at the University of Texas at Austin the Genome Sequencing and Analysis Facility (GSAF). Read sequences have been deposited into the NCBI Sequence Read Archive (PRJNA601748).

Quantification and Statistical Analysis

Read processing

Raw reads were used to generate Consensus Sequence Reads (CSR) using custom Python scripts that carried out the following steps. First, the beginning of each read was evaluated for the presence of the expected 5′-end tag, consisting of a random 12-base unique molecular identifier (UMI) followed by four fixed bases (5′-N_{12}CAGT). Read pairs lacking the correct 5′-end tag on either read were discarded. Across all samples, 80.2% of read pairs had both UMIs. For remaining read pairs, the UMIs found on each end were concatenated to create a 24-base dual-UMI that uniquely identifies the original DNA fragment that was amplified and sequenced. To group all reads corresponding to the same initial DNA molecule, a FASTA file of all dual-UMIs was used as input into the *ustacks* program from the Stacks software pipeline (Version 1.48) (Catchen et al., 2013) with the following options: a single read was sufficient to seed a stack, a single mismatch within the dual-UMI was allowed in assigning a read to a stack, secondary reads and haplotypes were disabled, and stacks with high coverage were preserved. Then, CSRs were generated for all dual-UMI groups sequenced at least twice by taking the straight consensus of all reads that were merged into that stack. If no base exceeded 50% frequency at a given position in this set of reads, then that base was set as unknown (N). Of the read pairs with valid dual-UMIs, 41.6% were incorporated into consensus reads across all samples. The average number of dual-UMI read pairs utilized to create each consensus read was 2.46, which gives an overall yield of consensus reads per read in a pair with a valid dual-UMI 16.9%.

Variant calling

We used the *breseq* pipeline (Barrick et al., 2014; Deatherage and Barrick, 2014; Deatherage et al., 2015) (version 0.26.0) to call single-nucleotide variants (SNVs) and structural variants (SVs) from the CSRs. This pipeline used Bowtie2 (version 2.2.5) for read mapping (Langmead and Salzberg, 2012). We divided the genome sequence of the ancestral *E. coli* REL606 strain into two types of reference regions for mapping in this analysis. The eight regions of the genome tiled with probes—extended with hundreds of bases of flanking sequence on both sides—were input as "targeted" sequences, and the remainder of the genome with the identical eight regions masked to degenerate N bases was supplied as a "junction-only" reference (to which reads are mapped without variant calling). All 116 samples were analyzed using *breseq* in polymorphism prediction mode with all bias, minimum allele frequency, and read-count filters disabled. Evidence items in the Genome Diff (GD) files for all samples were combined using the *gdtools* utility program to generate a single merged GD file with each piece of evidence listed a single time, regardless of how many times it was detected in different samples. We then re-ran *breseq* using the same parameters except that this GD file was supplied as an input user-evidence file to force output of variant and reference information for these putative variants in every sample. Then, we extracted the number of variant reads supporting each putative variant allele and the total number of reads at that reference location from the GD file output by *breseq*. Subsequent statistical tests and fitting steps were performed in R (version 4.0.0) (R Core Team, 2016) using the ggplot2 package for data visualization (Wickham, 2016).

Since this original analysis was conducted at the level of *breseq* evidence (i.e., single columns of read pileups on the reference genome or instances of new sequence junctions), we next merged sets of observations that were consistent with a single mutational event when they also had frequency trajectories that tracked together. For example, a three-base deletion has

778 separate evidence items for the first, second, and third missing bases at this stage in the analysis.
779 To identify candidates for merging evidence into a single mutational event, we analyzed data
780 from each complete time course (generation 30 to 530) and selective sweep window (generation
781 163 to 243) separately. We only considered mutations that exceeded a threshold frequency of
782 0.03% at some time during each time course as candidates for merging.
783 Read alignment (RA) evidence items were merged when they were located within 6 base
784 pairs of one another and the normalized Canberra distance between the vectors of their frequency
785 observations across all time points was ≤ 0.1. All RA evidence pairs of this kind were found to
786 co-occur in the same sequencing reads. For these cases, the read counts for the first linked
787 mutation were used to represent the entire event. For example, if a deletion of three base pairs
788 was predicted from evidence of missing bases at positions x, y, and z; then the frequency of
789 missing the first base (x) was assigned to the entire three-base deletion mutation.
790 For new junction (JC) evidence we performed the same merging procedure but allowed
791 linked mutations to be within a larger window of 20 base pairs and within a normalized Canberra
792 distance of 0.5. JC pairs passing these criteria were only merged if they were also consistent with
793 an IS-element insertion in terms of their relative orientation and spacing. In this case the variant
794 and total read counts were added together for the two different junctions, as the junctions on each
795 side of the inserted IS element provide independent information for estimating the frequency of
796 this type of mutation. We allowed unpaired JC evidence passing the filters to also predict IS
797 element mutations. This situation may indicate that there was an IS-mediated deletion between
798 an element that inserted within the gene and another element from the same family located
799 outside of the targeted region or more complex chromosomal rearrangements involving a newly
800 inserted IS element (Raeside et al., 2014).

Time course filtering and fitness effect estimation

After merging evidence of genetic variants into lists of putative mutations, we further eliminated some of these from consideration using several filtering steps. For the complete time courses, we first required that non-zero frequencies be observed for a mutation in samples from two different time points. We next applied a filter to eliminate spurious variants that can be recognized as arising from systematic sequencing or read alignment errors because they do not exhibit the correlated changes in frequency over time expected for the frequency trajectories of real mutations (Lang et al., 2013). Specifically, we required that the time-series of estimated frequencies for a mutation over all analyzed time points have an autocorrelation value ≥ 0.55.

For the analysis of mutation trajectories during the selective sweep window, we eliminated putative mutations for which there was great uncertainty in the estimated fitness effect or evidence that its trajectory reflected multiple beneficial mutations occurring in the same genome. Specifically, we required that a mutation was first observed at generation 196 or earlier and that its estimated frequency was $\geq 10^{-4}$ in every sample that was sequenced from generation 223 to 243. Then, we fit a binomial logistic model with slope and *y*-intercept terms to the time courses of counts of variant and reference (total minus variant) observations for each mutation. We used a negative offset in the model of the number of generations up to each time point so that the slope represents one plus the selection coefficient that is characteristic of the subpopulation with that mutation. We filtered out any mutations for which this fit had an AIC < 200, a *p*-value for the slope differing from zero of > 0.005, or a *y*-intercept < -20. The fitness effects that we report for mutations are the selection coefficients fit from the model divided by the natural logarithm of two so that they are expressed per generations of binary cell division. One plus the fitness effect

824 is the relative fitness of a cell with that mutation. These values can be directly compared to
825 experimental measurements of relative fitness and mutation fitness effects made using co-culture
826 competition assays (Lenski et al., 1991; Tenaillon et al., 2016).
827 This procedure for determining fitness effects assumes that the trajectories reflect
828 competition purely against the ancestral strain. However, we detected a consistent deviation from
829 linearity for all mutation trajectories after generation 196. The rates at which the frequencies of
830 all mutations were increasing decelerated, indicating that the overall population fitness had
831 improved to a degree that it reduced their effective advantage versus their competitors. To
832 account for this change we fit additional parameters defining a stepwise increase in the average
833 relative fitness of the population within each interval between sequenced samples from
834 generation 196 onward. The increase in population fitness reduces the effective time basis used
835 in the model to determine the slope to the number of generations in each interval divided by the
836 average relative fitness during that interval. We determined the population fitness values that
837 minimized the AIC of this modified binomial logistic model. The figures show the best stepwise
838 increases in population fitness between the sequenced time points from generation 196 onward
839 fitting to the trajectories of all mutations in a given population at the same time. We performed
840 1000 bootstrap resamplings of the mutations in each population to estimate 95% confidence
841 intervals on the estimated population fitness values in each interval for that population.
842 We combined information across multiple populations in two ways to further improve the
843 estimates of mutation fitness effects. First, there was considerable uncertainty in the estimates of
844 the stepwise population fitness increases for each population considered alone. Because the
845 actual population fitness trajectories of all populations are expected to be highly similar to one
846 another, we fit a consensus stepwise increase in population fitness over time that best improved

the fits for all mutations from all populations. Second, we observed 27 cases in which the exact same change in a gene's sequence was observed and passed our filtering criteria in multiple experimental populations. Because each population was started from single cells, we can be sure that these are independent observations of the same mutation. Therefore, we fit one consensus fitness effect (slope) for each of these recurrent mutations across all populations. We still allowed the *y*-intercept for each of these mutations to vary from population to population because this parameter is related to how early the mutation evolved, which is expected to be different in each replicate population.

Protein structure analysis

Structural domains in NadR, PykF, and TopA were defined according to UniProt and papers reporting x-ray crystal structures. Mutations in PykF were mapped onto Protein Data Bank structure 4YNG (Donovan et al., 2016). Mutations in TopA were mapped onto Protein Data Bank structure 1MW8 (Perry and Mondragón, 2003). Protein structures were visualized using Pymol v2.3.5 (Schrödinger LLC).

REFERENCES

Bainbridge, M.N., Wang, M., Burgess, D.L., Kovar, C., Rodesch, M.J., D'Ascenzo, M., Kitzman, J., Wu, Y.-Q., Newsham, I., Richmond, T.A., et al. (2010). Whole exome capture in solution with 3 Gbp of data. Genome Biol. *11*, R62.

Barrick, J.E. (2020). Limits to predicting evolution: insights from a long-term experiment with *Escherichia coli*. In Evolution in Action: Past, Present and Future, W. Banzhaf, B.H.C. Cheng, K. Deb, K.E. Holekamp, R.E. Lenski, C. Ofria, R.T. Pennock, W.F. Punch, and D.J. Whittaker, eds. (Cham: Springer), pp. 63–76.

Barrick, J.E., and Lenski, R.E. (2009). Genome-wide mutational diversity in an evolving population of *Escherichia coli*. Cold Spring Harb. Symp. Quant. Biol. *74*, 119–129.

Barrick, J.E., and Lenski, R.E. (2013). Genome dynamics during experimental evolution. Nat. Rev. Genet. *14*, 827–839.

Barrick, J.E., Yu, D.S., Yoon, S.H., Jeong, H., Oh, T.K., Schneider, D., Lenski, R.E., and Kim, J.F. (2009). Genome evolution and adaptation in a long-term experiment with *Escherichia coli*. Nature *461*, 1243–1247.

Barrick, J.E., Colburn, G., Deatherage, D.E., Traverse, C.C., Strand, M.D., Borges, J.J., Knoester, D.B., Reba, A., and Meyer, A.G. (2014). Identifying structural variation in haploid microbial genomes from short-read resequencing data using *breseq*. BMC Genomics *15*, 1039.

Baym, M., Lieberman, T.D., Kelsic, E.D., Chait, R., Gross, R., Yelin, I., and Kishony, R. (2016). Spatiotemporal microbial evolution on antibiotic landscapes. Science *353*, 1147–1151.

Blundell, J.R., and Levy, S.F. (2014). Beyond genome sequencing: Lineage tracking with barcodes to study the dynamics of evolution, infection, and cancer. Genomics *104*, 417–430.

Camacho, C., Coulouris, G., Avagyan, V., Ma, N., Papadopoulos, J., Bealer, K., and Madden, T.L. (2009). BLAST+: architecture and applications. BMC Bioinformatics *10*, 421.

Catchen, J., Hohenlohe, P.A., Bassham, S., Amores, A., and Cresko, W.A. (2013). Stacks: an analysis tool set for population genomics. Mol. Ecol. *22*, 3124–3140.

Chou, H.-H., Chiu, H.-C., Delaney, N.F., Segrè, D., and Marx, C.J. (2011). Diminishing returns epistasis among beneficial mutations decelerates adaptation. Science *332*, 1190–1192.

Chubiz, L.M., Lee, M.-C., Delaney, N.F., and Marx, C.J. (2012). FREQ-Seq: a rapid, cost-effective, sequencing-based method to determine allele frequencies directly from mixed populations. PLoS ONE *7*, e47959.

Crozat, E., Philippe, N., Lenski, R.E., Geiselmann, J., and Schneider, D. (2005). Long-term experimental evolution in *Escherichia coli*. XII. DNA topology as a key target of selection. Genetics *169*, 523–532.

Crozat, E., Winkworth, C., Gaffé, J., Hallin, P.F., Riley, M.A., Lenski, R.E., and Schneider, D. (2010). Parallel genetic and phenotypic evolution of DNA superhelicity in experimental populations of *Escherichia coli*. Mol. Biol. Evol. *27*, 2113–2128.

Cvijović, I., Nguyen Ba, A.N., and Desai, M.M. (2018). Experimental studies of evolutionary

dynamics in microbes. Trends Genet. *34*, 693–703.

Deatherage, D.E., and Barrick, J.E. (2014). Identification of mutations in laboratory-evolved microbes from next-generation sequencing data using *breseq*. Methods Mol. Biol. *1151*, 165–188.

Deatherage, D.E., Traverse, C.C., Wolf, L.N., and Barrick, J.E. (2015). Detecting rare structural variation in evolving microbial populations from new sequence junctions using *breseq*. Front. Genet. *5*, 468.

Deatherage, D.E., Kepner, J.L., Bennett, A.F., Lenski, R.E., and Barrick, J.E. (2017). Specificity of genome evolution in experimental populations of *Escherichia coli* evolved at different temperatures. Proc. Natl. Acad. Sci. U. S. A. *114*, E1904–E1912.

Desai, M.M., Walczak, A.M., and Fisher, D.S. (2012). Genetic diversity and the structure of genealogies in rapidly adapting populations. Genetics *193*, 565–585.

Dinardo, S., Voelkel, K.A., Sternglanz, R., Reynolds, A.E., and Wright, A. (1982). *Escherichia coli* DNA topoisomerase I mutants have compensatory mutations in DNA gyrase genes. Cell *31*, 43–51.

Ding, L., Ley, T.J., Larson, D.E., Miller, C.A., Koboldt, D.C., Welch, J.S., Ritchey, J.K., Young, M.A., Lamprecht, T., McLellan, M.D., et al. (2012). Clonal evolution in relapsed acute myeloid leukaemia revealed by whole-genome sequencing. Nature *481*, 506–510.

Donovan, K.A., Atkinson, S.C., Kessans, S.A., Peng, F., Cooper, T.F., Griffin, M.D.W., Jameson, G.B., and Dobson, R.C.J. (2016). Grappling with anisotropic data, pseudo-merohedral twinning and pseudo-translational noncrystallographic symmetry: A case study involving pyruvate kinase. Acta Crystallogr. Sect. D Struct. Biol. *72*, 512–519.

Fischer, S., Greipel, L., Klockgether, J., Dorda, M., Wiehlmann, L., Cramer, N., and Tümmler, B. (2017). Multilocus amplicon sequencing of *Pseudomonas aeruginosa* cystic fibrosis airways isolates collected prior to and after early antipseudomonal chemotherapy. J. Cyst. Fibros. *16*, 346–352.

Fowler, D.M., and Fields, S. (2014). Deep mutational scanning: a new style of protein science. Nat. Methods *11*, 801–807.

Frenkel, E.M., McDonald, M.J., Van Dyken, J.D., Kosheleva, K., Lang, G.I., and Desai, M.M. (2015). Crowded growth leads to the spontaneous evolution of semistable coexistence in laboratory yeast populations. Proc. Natl. Acad. Sci. *112*, 11306–11311.

Furusawa, C., Horinouchi, T., and Maeda, T. (2018). Toward prediction and control of antibiotic-resistance evolution. Curr. Opin. Biotechnol. *54*, 45–49.

Garst, A.D., Bassalo, M.C., Pines, G., Lynch, S.A., Halweg-Edwards, A.L., Liu, R., Liang, L., Wang, Z., Zeitoun, R., Alexander, W.G., et al. (2017). Genome-wide mapping of mutations at single-nucleotide resolution for protein, metabolic and genome engineering. Nat. Biotechnol. *35*, 48–55.

Genovese, G., Kähler, A.K., Handsaker, R.E., Lindberg, J., Rose, S.A., Bakhoum, S.F., Chambert, K., Mick, E., Neale, B.M., Fromer, M., et al. (2014). Clonal hematopoiesis and blood-cancer risk inferred from blood DNA sequence. N. Engl. J. Med. *371*, 2477–2487.

Gerrish, P.J., and Lenski, R.E. (1998). The fate of competing beneficial mutations in an asexual population. Genetica *102–103*, 127–144.

Good, B.H., McDonald, M.J., Barrick, J.E., Lenski, R.E., and Desai, M.M. (2017). The dynamics of molecular evolution over 60,000 generations. Nature *551*, 45–50.

Gresham, D., and Dunham, M.J. (2014). The enduring utility of continuous culturing in experimental evolution. Genomics *104*, 399–405.

Hegreness, M., and Kishony, R. (2007). Analysis of genetic systems using experimental evolution and whole-genome sequencing. Genome Biol. *8*, 201.

Hegreness, M., Shoresh, N., Hartl, D., and Kishony, R. (2006). An equivalence principle for the incorporation of favorable mutations in asexual populations. Science *311*, 1615–1617.

Hong, J., and Gresham, D. (2017). Incorporation of unique molecular identifiers in TruSeq adapters improves the accuracy of quantitative sequencing. Biotechniques *63*, 221–226.

Hong, J., Brandt, N., Abdul-Rahman, F., Yang, A., Hughes, T., and Gresham, D. (2018). An incoherent feedforward loop facilitates adaptive tuning of gene expression. eLife *7*, e32323.

Houdaigui, B. El, Forquet, R., Hindré, T., Schneider, D., Nasser, W., Reverchon, S., and Meyer, S. (2019). Bacterial genome architecture shapes global transcriptional regulation by DNA supercoiling. Nucleic Acids Res. *47*, 5648–5657.

Jeong, H., Barbe, V., Lee, C.H., Vallenet, D., Yu, D.S., Choi, S.-H., Couloux, A., Lee, S.-W., Yoon, S.H., Cattolico, L., et al. (2009). Genome sequences of *Escherichia coli* B strains REL606 and BL21(DE3). J. Mol. Biol. *394*, 644–652.

Khan, A.I., Dinh, D.M., Schneider, D., Lenski, R.E., and Cooper, T.F. (2011). Negative epistasis between beneficial mutations in an evolving bacterial population. Science *332*, 1193–1196.

Kivioja, T., Vähärautio, A., Karlsson, K., Bonke, M., Enge, M., Linnarsson, S., and Taipale, J. (2012). Counting absolute numbers of molecules using unique molecular identifiers. Nat. Methods *9*, 72–74.

Kochanowski, K., Volkmer, B., Gerosa, L., Van Rijsewijk, B.R.H., Schmidt, A., and Heinemann, M. (2013). Functioning of a metabolic flux sensor in *Escherichia coli*. Proc. Natl. Acad. Sci. U. S. A. *110*, 1130–1135.

Kryazhimskiy, S., Rice, D.P., Jerison, E.R., and Desai, M.M. (2014). Global epistasis makes adaptation predictable despite sequence-level stochasticity. Science *344*, 1519–1522.

Kurnasov, O. V., Polanuyer, B.M., Ananta, S., Sloutsky, R., Tam, A., Gerdes, S.Y., and Osterman, A.L. (2003). Ribosylnicotinamide Kinase Domain of NadR Protein: Identification and Implications in NAD Biosynthesis. J. Bacteriol. *185*, 698–698.

Landau, D.A., Carter, S.L., Stojanov, P., McKenna, A., Stevenson, K., Lawrence, M.S., Sougnez, C., Stewart, C., Sivachenko, A., Wang, L., et al. (2013). Evolution and impact of subclonal mutations in chronic lymphocytic leukemia. Cell *152*, 714–726.

Lang, G.I., Rice, D.P., Hickman, M.J., Sodergren, E., Weinstock, G.M., Botstein, D., and Desai, M.M. (2013). Pervasive genetic hitchhiking and clonal interference in forty evolving yeast populations. Nature *500*, 571–574.

Langmead, B., and Salzberg, S.L. (2012). Fast gapped-read alignment with Bowtie 2. Nat. Methods *9*, 357–360.

Lee, S.Y., and Kim, H.U. (2015). Systems strategies for developing industrial microbial strains. Nat. Biotechnol. *33*, 1061–1072.

Lenski, R.E., and Travisano, M. (1994). Dynamics of adaptation and diversification: a 10,000-generation experiment with bacterial populations. Proc. Natl. Acad. Sci. U. S. A. *91*, 6808–6814.

Lenski, R.E., Rose, M.R., Simpson, S.C., and Tadler, S.C. (1991). Long-term experimental evolution in *Escherichia coli*. I. Adaptation and divergence during 2,000 generations. Am. Nat. *138*, 1315–1341.

Levy, S.F., Blundell, J.R., Venkataram, S., Petrov, D.A., Fisher, D.S., and Sherlock, G. (2015). Quantitative evolutionary dynamics using high-resolution lineage tracking. Nature *519*, 181–186.

Lind, P.A., Farr, A.D., and Rainey, P.B. (2015). Experimental evolution reveals hidden diversity in evolutionary pathways. eLife *4*, e07074.

Maddamsetti, R., Lenski, R.E., and Barrick, J.E. (2015). Adaptation, clonal interference, and frequency-dependent interactions in a long-term evolution experiment with *Escherichia coli*. Genetics *200*, 619–631.

Marusyk, A., Almendro, V., and Polyak, K. (2012). Intra-tumour heterogeneity: A looking glass for cancer? Nat. Rev. Cancer *12*, 323–334.

Marvig, R.L., Sommer, L.M., Molin, S., and Johansen, H.K. (2015). Convergent evolution and adaptation of *Pseudomonas aeruginosa* within patients with cystic fibrosis. Nat. Genet. *47*, 57–64.

Massé, E., and Drolet, M. (1999). Relaxation of transcription-induced negative supercoiling is an essential function of *Escherichia coli* DNA topoisomerase I. J. Biol. Chem. *274*, 16654–16658.

Mattevi, A., Valentini, G., Rizzi, M., Speranza, M.L., Bolognesi, M., and Coda, A. (1995). Crystal structure of *Escherichia coli* pyruvate kinase type I: molecular basis of the allosteric transition. Structure *3*, 729–741.

McDonald, M.J. (2019). Microbial experimental evolution – a proving ground for evolutionary theory and a tool for discovery. EMBO Rep. *20*, e46992.

Merlo, L.M.F., Pepper, J.W., Reid, B.J., and Maley, C.C. (2006). Cancer as an evolutionary and ecological process. Nat. Rev. Cancer *6*, 924–935.

Merlo, L.M.F., Shah, N.A., Li, X., Blount, P.L., Vaughan, T.L., Reid, B.J., and Maley, C.C. (2010). A comprehensive survey of clonal diversity measures in Barrett's esophagus as biomarkers of progression to esophageal adenocarcinoma. Cancer Prev. Res. (Phila). *3*, 1388–1397.

Newman, A.M., Bratman, S. V., To, J., Wynne, J.F., Eclov, N.C.W., Modlin, L.A., Liu, C.L., Neal, J.W., Wakelee, H.A., Merritt, R.E., et al. (2014). An ultrasensitive method for quantitating circulating tumor DNA with broad patient coverage. Nat. Med. *20*, 548–554.

Newman, A.M., Lovejoy, A.F., Klass, D.M., Kurtz, D.M., Chabon, J.J., Scherer, F., Stehr, H., Liu, C.L., Bratman, S. V., Say, C., et al. (2016). Integrated digital error suppression for improved

1021 detection of circulating tumor DNA. Nat. Biotechnol. *34*, 547–555.

1022 Nielsen, J., and Keasling, J.D. (2016). Engineering cellular metabolism. Cell *164*, 1185–1197.

1023 van Opijnen, T., and Camilli, A. (2013). Transposon insertion sequencing: a new tool for
1024 systems-level analysis of microorganisms. Nat. Rev. Microbiol. *11*, 435–442.

1025 Ostrowski, E.A., Woods, R.J., and Lenski, R.E. (2008). The genetic basis of parallel and
1026 divergent phenotypic responses in evolving populations of *Escherichia coli*. Proc. R. Soc. B *275*,
1027 277–284.

1028 Park, S.-C., and Krug, J. (2007). Clonal interference in large populations. Proc. Natl. Acad. Sci.
1029 U. S. A. *104*, 18135–18140.

1030 Peng, F., Widmann, S., Wünsche, A., Duan, K., Donovan, K.A., Dobson, R.C.J., Lenski, R.E.,
1031 and Cooper, T.F. (2018). Effects of beneficial mutations in *pykF* gene vary over time and across
1032 replicate populations in a long-term experiment with bacteria. Mol. Biol. Evol. *35*, 202–210.

1033 Perry, K., and Mondragón, A. (2003). Structure of a complex between *E. coli* DNA
1034 topoisomerase I and single-stranded DNA. Structure *11*, 1349–1358.

1035 Phaneuf, P. V., Yurkovich, J.T., Heckmann, D., Wu, M., Sandberg, T.E., King, Z.A., Tan, J.,
1036 Palsson, B.O., and Feist, A.M. (2020). Causal mutations from adaptive laboratory evolution are
1037 outlined by multiple scales of genome annotations and condition-specificity. BMC Genomics *21*,
1038 514.

1039 Pruss, G.J., Manes, S.H., and Drlica, K. (1982). *Escherichia coli* DNA topoisomerase I mutants:
1040 Increased supercoiling is corrected by mutations near gyrase genes. Cell *31*, 35–42.

1041 R Core Team (2016). R: A Language and Environment for Statistical Computing (Vienna,
1042 Austria: R Foundation for Statistical Computing). http://www.R-project.org/

1043 Raeside, C., Gaffé, J., Deatherage, D.E., Tenaillon, O., Briska, A.M., Ptashkin, R.N., Cruveiller,
1044 S., Médigue, C., Lenski, R.E., Barrick, J.E., et al. (2014). Large chromosomal rearrangements
1045 during a long-term evolution experiment with *Escherichia coli*. MBio *5*, e01377-14.

1046 Raffaelli, N., Lorenzi, T., Mariani, P.L., Emanuelli, M., Amici, A., Ruggieri, S., and Magni, G.
1047 (1999). The *Escherichia coli* NadR regulator is endowed with nicotinamide mononucleotide
1048 adenylyltransferase activity. J. Bacteriol. *181*, 5509–5511.

1049 Rainey, P.B., Remigi, P., Farr, A.D., and Lind, P.A. (2017). Darwin was right: where now for
1050 experimental evolution? Curr. Opin. Genet. Dev. *47*, 102–109.

1051 Renda, B.A., Hammerling, M.J., and Barrick, J.E. (2014). Engineering reduced evolutionary
1052 potential for synthetic biology. Mol. Biosyst. *10*, 1668–1678.

1053 Rugbjerg, P., and Sommer, M.O.A. (2019). Overcoming genetic heterogeneity in industrial
1054 fermentations. Nat. Biotechnol. *37*, 869–876.

1055 Rugbjerg, P., Myling-Petersen, N., Porse, A., Sarup-Lytzen, K., and Sommer, M.O.A. (2018).
1056 Diverse genetic error modes constrain large-scale bio-based production. Nat. Commun. *9*, 787.

1057 Ryall, B., Eydallin, G., and Ferenci, T. (2012). Culture history and population heterogeneity as
1058 determinants of bacterial adaptation: the adaptomics of a single environmental transition.

Microbiol. Mol. Biol. Rev. *76*, 597–625.

Sandoval, C.M., Ayson, M., Moss, N., Lieu, B., Jackson, P., Gaucher, S.P., Horning, T., Dahl, R.H., Denery, J.R., Abbott, D.A., et al. (2014). Use of pantothenate as a metabolic switch increases the genetic stability of farnesene producing *Saccharomyces cerevisiae*. Metab. Eng. *25*, 215–226.

Schmitt, M.W., Kennedy, S.R., Salk, J.J., Fox, E.J., Hiatt, J.B., and Loeb, L.A. (2012). Detection of ultra-rare mutations by next-generation sequencing. Proc. Natl. Acad. Sci. U. S. A. *109*, 14508–14513.

Siddiquee, K.A.Z., Arauzo-Bravo, M.J., and Shimizu, K. (2004). Effect of a pyruvate kinase (*pykF*-gene) knockout mutation on the control of gene expression and metabolic fluxes in *Escherichia coli*. FEMS Microbiol. Lett. *235*, 25–33.

Stefani, S., Campana, S., Cariani, L., Carnovale, V., Colombo, C., Lleo, M.M., Iula, V.D., Minicucci, L., Morelli, P., Pizzamiglio, G., et al. (2017). Relevance of multidrug-resistant *Pseudomonas aeruginosa* infections in cystic fibrosis. Int. J. Med. Microbiol. *307*, 353–362.

Tan, K., Zhou, Q., Cheng, B., Zhang, Z., Joachimiak, A., and Tse-Dinh, Y.C. (2015). Structural basis for suppression of hypernegative DNA supercoiling by *E. coli* topoisomerase I. Nucleic Acids Res. *43*, 11031–11046.

Tenaillon, O., Rodríguez-Verdugo, A., Gaut, R.L., McDonald, P., Bennett, A.F., Long, A.D., and Gaut, B.S. (2012). The molecular diversity of adaptive convergence. Science *335*, 457–461.

Tenaillon, O., Barrick, J.E., Ribeck, N., Deatherage, D.E., Blanchard, J.L., Dasgupta, A., Wu, G.C., Wielgoss, S., Cruveiller, S., Médigue, C., et al. (2016). Tempo and mode of genome evolution in a 50,000-generation experiment. Nature *536*, 165–170.

Thomas, R.K., Nickerson, E., Simons, J.F., Jänne, P.A., Tengs, T., Yuza, Y., Garraway, L.A., LaFramboise, T., Lee, J.C., Shah, K., et al. (2006). Sensitive mutation detection in heterogeneous cancer specimens by massively parallel picoliter reactor sequencing. Nat. Med. *12*, 852–855.

Traverse, C.C., Mayo-Smith, L.M., Poltak, S.R., and Cooper, V.S. (2013). Tangled bank of experimentally evolved *Burkholderia* biofilms reflects selection during chronic infections. Proc. Natl. Acad. Sci. U. S. A. *110*, E250–E259.

Venkataram, S., Dunn, B., Li, Y., Agarwala, A., Chang, J., Ebel, E.R., Geiler-Samerotte, K., Hérissant, L., Blundell, J.R., Levy, S.F., et al. (2016). Development of a comprehensive genotype-to-fitness map of adaptation-driving mutations in yeast. Cell *166*, 1585-1596.E22.

Watson, C.J., Papula, A.L., Poon, G.Y.P., Wong, W.H., Young, A.L., Druley, T.E., Fisher, D.S., and Blundell, J.R. (2020). The evolutionary dynamics and fitness landscape of clonal hematopoiesis. Science *367*, 1449–1454.

Wei, X., and Zhang, J. (2019). Patterns and mechanisms of diminishing returns from beneficial mutations. Mol. Biol. Evol. *36*, 1008–1021.

Wickham, H. (2016). ggplot2: Elegant Graphics for Data Analysis (New York: Springer-Verlag).

Winstanley, C., O'Brien, S., and Brockhurst, M.A. (2016). *Pseudomonas aeruginosa* evolutionary adaptation and diversification in cystic fibrosis chronic lung infections. Trends

Microbiol. *24*, 327–337.

Wiser, M.J., Ribeck, N., and Lenski, R.E. (2013). Long-term dynamics of adaptation in asexual populations. Science *342*, 1364–1367.

Woods, R., Schneider, D., Winkworth, C.L., Riley, M.A., and Lenski, R.E. (2006). Tests of parallel molecular evolution in a long-term experiment with *Escherichia coli*. Proc. Natl. Acad. Sci. U. S. A. *103*, 9107–9712.

Woods, R.J., Barrick, J.E., Cooper, T.F., Shrestha, U., Kauth, M.R., and Lenski, R.E. (2011). Second-order selection for evolvability in a large *Escherichia coli* population. Science *331*, 1433–1436.

Zelder, O., and Hauer, B. (2000). Environmentally directed mutations and their impact on industrial biotransformation and fermentation processes. Curr. Opin. Microbiol. *3*, 248–251.

KEY RESOURCES TABLE

REAGENT or RESOURCE	SOURCE	IDENTIFIER
Chemicals, peptides, and recombinant proteins		
Klenow fragment exo$^-$	New England Biolabs	M0212S
MyOne Streptavidin C1 Dynabeads	Life Technologies	65001
Critical commercial assays		
PureLink Genomic DNA Mini kit	Life Technologies	K210011
LTP Library Preparation Kit	Kappa Biosystems	Kk8232
SeqCap EZ Hybridization and Wash Kit	NimbleGen	05 634 261 001
KAPA Library Amplification Kit	Kappa Biosystems	KK2611
Deposited data		
Raw Illumina Sequencing Data	This paper	NCBI SRA: PRJNA601748
Experimental models: Organisms/strains		
E. coli: Strain background: REL606	Lenski et al., 1991	N/A
E. coli: Strain background: REL607	Lenski et al., 1991	N/A
Oligonucleotides		
21 Illumina Sequencing Adapters containing 12-base MI: See Table S1	This paper	N/A
242 60-base xGen Lockdown probes: see Table S2	This paper	N/A
2 Blocking Oligos: see Table S3	This paper	N/A
Software and algorithms		
BLASTN	Camacho et al., 2009	https://blast.ncbi.nlm.nih.gov/Blast.cgi
CSR generation python script	This paper	DOI: 10.5281/zenodo.5092871
Stacks v1.48	Catchen et al., 2013	https://catchenlab.life.illinois.edu/stacks/
breseq v0.26.0	Deatherage and Barrick, 2014	https://github.com/barricklab/breseq
Bowtie2 v2.2.5	Langmead and Salzberg, 2012	http://bowtie-bio.sourceforge.net/bowtie2/index.shtml
R v4.0.0	R Core Team, 2016	https://www.r-project.org/
Custom *breseq* post-processing Python script	This paper	DOI: 10.5281/zenodo.5092871
Statistical testing and modeling of trajectories R script	This paper	DOI: 10.5281/zenodo.5092871
Pymol v2.3.5	Schrodinger LLC	Pymol.org
Pymol figure visualization script	This paper	DOI: 10.5281/zenodo.5092871
Other		
REL606.6.GENES.1400-flanking.gff3	This paper	DOI: 10.5281/zenodo.5092871

REL606.6.GENES.MASKED.gff3	This paper	DOI: 10.5281/zenodo.5092871

Table S1. Adapter sequences

Name	Sequence
UTBC52	/5Phos/ACTG**NNNNNNNNNNNN**AGATCGGAAGAGCACACGTCTGAACTCCAGTCAC**AACATA**ATCTCGTATGCCGTCTTCTCGTTG
UTBC75	/5Phos/ACTG**NNNNNNNNNNNN**AGATCGGAAGAGCACACGTCTGAACTCCAGTCAC**ACGCCG**ATCTCGTATGCCGTCTTCTCGTTG
TSBC25	/5Phos/ACTG**NNNNNNNNNNNN**AGATCGGAAGAGCACACGTCTGAACTCCAGTCAC**ACTGAT**ATCTCGTATGCCGTCTTCTCGTTG
TSBC14	/5Phos/ACTG**NNNNNNNNNNNN**AGATCGGAAGAGCACACGTCTGAACTCCAGTCAC**AGTTCC**ATCTCGTATGCCGTCTTCTCGTTG
UTBC64	/5Phos/ACTG**NNNNNNNNNNNN**AGATCGGAAGAGCACACGTCTGAACTCCAGTCAC**ATACGA**ATCTCGTATGCCGTCTTCTCGTTG
TSBC34	/5Phos/ACTG**NNNNNNNNNNNN**AGATCGGAAGAGCACACGTCTGAACTCCAGTCAC**CATGGC**ATCTCGTATGCCGTCTTCTCGTTG
TSBC36	/5Phos/ACTG**NNNNNNNNNNNN**AGATCGGAAGAGCACACGTCTGAACTCCAGTCAC**CCAACA**ATCTCGTATGCCGTCTTCTCGTTG
UTBC63	/5Phos/ACTG**NNNNNNNNNNNN**AGATCGGAAGAGCACACGTCTGAACTCCAGTCAC**CCCCAC**ATCTCGTATGCCGTCTTCTCGTTG
TSBC37	/5Phos/ACTG**NNNNNNNNNNNN**AGATCGGAAGAGCACACGTCTGAACTCCAGTCAC**CGGAAT**ATCTCGTATGCCGTCTTCTCGTTG
UTBC58	/5Phos/ACTG**NNNNNNNNNNNN**AGATCGGAAGAGCACACGTCTGAACTCCAGTCAC**CGGTTA**ATCTCGTATGCCGTCTTCTCGTTG
TSBC23	/5Phos/ACTG**NNNNNNNNNNNN**AGATCGGAAGAGCACACGTCTGAACTCCAGTCAC**GAGTGG**ATCTCGTATGCCGTCTTCTCGTTG
TSBC09	/5Phos/ACTG**NNNNNNNNNNNN**AGATCGGAAGAGCACACGTCTGAACTCCAGTCAC**GATCAG**ATCTCGTATGCCGTCTTCTCGTTG
UTBC86	/5Phos/ACTG**NNNNNNNNNNNN**AGATCGGAAGAGCACACGTCTGAACTCCAGTCAC**GGCGGT**ATCTCGTATGCCGTCTTCTCGTTG
TSBC20	/5Phos/ACTG**NNNNNNNNNNNN**AGATCGGAAGAGCACACGTCTGAACTCCAGTCAC**GTGGCC**ATCTCGTATGCCGTCTTCTCGTTG
UTBC69	/5Phos/ACTG**NNNNNNNNNNNN**AGATCGGAAGAGCACACGTCTGAACTCCAGTCAC**GTTATT**ATCTCGTATGCCGTCTTCTCGTTG
UTBC56	/5Phos/ACTG**NNNNNNNNNNNN**AGATCGGAAGAGCACACGTCTGAACTCCAGTCAC**TAAGAA**ATCTCGTATGCCGTCTTCTCGTTG
TSBC10	/5Phos/ACTG**NNNNNNNNNNNN**AGATCGGAAGAGCACACGTCTGAACTCCAGTCAC**TAGCTT**ATCTCGTATGCCGTCTTCTCGTTG
TSBC45	/5Phos/ACTG**NNNNNNNNNNNN**AGATCGGAAGAGCACACGTCTGAACTCCAGTCAC**TCATTC**ATCTCGTATGCCGTCTTCTCGTTG
UTBC51	/5Phos/ACTG**NNNNNNNNNNNN**AGATCGGAAGAGCACACGTCTGAACTCCAGTCAC**TGAAGG**ATCTCGTATGCCGTCTTCTCGTTG
UTBC94	/5Phos/ACTG**NNNNNNNNNNNN**AGATCGGAAGAGCACACGTCTGAACTCCAGTCAC**TTCTAT**ATCTCGTATGCCGTCTTCTCGTTG
Univ-F	AATGATACGGCGACCACCGAGATCTACACTCTTTCCCTACACGAC**GCTCTTCCGATCT**

/5Phos/ indicates that an oligonucleotide was chemically synthesized with a 5′ monophosphate. **Red bases** are sample barcodes. **Blue bases** are unique molecular identifiers (UMIs) that were synthesized with a mixture of all four bases at each N position. **Green bases** show where each sequence was individually annealed to Univ-F through the sequence and extended to make the double-stranded end of the adaptor that includes the unique molecular identifier before it was ligated to the DNA sample.

Table S2. Probe sequences

Name	Sequence	Start	End
ybaL_1	TATTTTTCATATTTTACATCCGGCAACCACCGTTTACCCCGTCACCACCTCACCCGCCGG	473596	473655
ybaL_2	TGGCGTTTCCAGCAGTTCCAGCATGGTACGGGCGATTTCACGCTCGCCCATCACTACCTG	473656	473715
ybaL_3	ATTCGCACCACGTTCGGTGATATACGCCACTTCATCGTCATAATGGGCGCGGGCAATAAT	473716	473775
ybaL_4	CTCAATATCCGGATTTTTCGCGCGGGCAGATGCCACAATCTCACCCGCTTCATAACCGTT	473776	473835
ybaL_5	GGGAATCGTCAGGATCAGCCATTTTGCACATTCCAGATGCGCCAGTTGCATAATTTCTTC	473836	473895
ybaL_6	GTTCGCCGCATTGCCCAATACTGCGCGGACCCCGCGCTCTCGCAGCTCATCAACACGGGT	473896	473955
ybaL_7	TCGTGACGTCTCAATCACCACCAGCGGAATATCAGAGGCGAGCAATTTCTCCCCCAGCAG	473956	474015
ybaL_8	GCTGCCTACACGACCGTAACCCACCAGTAGCGCATGGTTGCAAATATCCACTGGGATCTG	474016	474075
ybaL_9	CTTCTCTTCTTCGATTGCCTCTTCCAGCGTCTGCTCTTCCAGCGTTTCGGTCTTCGCCAG	474076	474135
ybaL_10	ATATTTCTCCAGTAGTGCGAACAGTACCGGGTTGAGCATAATCGACAGGATCGCCCCTGC	474136	474195
ybaL_11	CAGTACCAGGTTTTGTCCGGCCTGCGGCAGTAAATTCAATGCCATTCCCAGTCCCGCCAG	474196	474255
ybaL_12	GATAAACGCGAACTCACCAATCTGCGCCAGGCTGGCGGCGATGGTTAATGCCGTACGTTG	474256	474315
ybaL_13	GGAGTGACCAAACAGTCGCACCAGGAAAAATGCGGCTAACGACTTACCAAACAGAATAAT	474316	474375
ybaL_14	CGCCAGCGTCGCCAGCACTGCCAGCGGTTGCTGAATCAGAATTAACGGATCAAACAACAT	474376	474435
ybaL_15	CCCGACGGAGACAAAAAACAGCACCGCAAACGCGTCGCGCAATGGCAGCGTATCGTGGGC	474436	474495
ybaL_16	GGCACGGTGACTCAGTTCAGACTCGTTCAGTACCATCCCGGCAAAGAACGCACCGAGTGC	474496	474555
ybaL_17	AAAGGAGACATCAAACAGCTCTACCGCACCAAAGGCAACCCCTAACGCCAGCGCCAGCAC	474556	474615
ybaL_18	CGACAGGGTAAACAGCTCGCGAGAACCGGTTGCCGCGCTGCGTGCCATAATCCACGGCAC	474616	474675
ybaL_19	CAGACGGCGACCTACCAGCATCATAATGGCGATAAATGCGATCACTTTGCCGATGGTGAT	474676	474735
ybaL_20	CCCCATATCGACTGCAAGAGTGGCAAAGCCCACATCGCCCTGTTCCATCATTCCTGCCAC	474736	474795
ybaL_21	TGCGGGCAGCAACACCAGCGTCAGAACCATTACCAGGTCTTCCACAATCAACCAACCGAT	474796	474855
ybaL_22	GGCGATTTGCCCACGCTGACTGTCAATTAATTGCCGTTCTTCAAGTGCGCGCAGTAACAC	474856	474915
ybaL_23	CACGGTACTGGCGGTGGAAAGACATAAACCGAACACGATACCGGTCATTAACGACCAGCC	474916	474975
ybaL_24	CAGCACGGCAGAGAGCGCCATACCCAGCAGCGTCGCCACGGCTATCTGGGCGATCGCACC	474976	475035
ybaL_25	GGGAATGGCGATGGCCTTTACCGCCATCAAATCCTTCAGCGAAAAGTGCAAACCGACGCC	475036	475095
ybaL_26	AAACATCAACAGAATGACGCCCAGTTCAGCCAGTTCCGGGGCAAGCTTGGTATCGGCAAC	475096	475155
ybaL_27	AAAGCCCGGAGTGAATGGTCCTGCCAGCACACCCGCTAACAGATATCCCACCAGAGGAGA	475156	475215
ybaL_28	AATACGTAGTTTATTGGCCAGCATGCCGAGGATAAAGGCGAGCACAAGGCCGCCAACAAT	475216	475275
ybaL_29	GGTGGTGATAAGCGGGGTGGCGTGATGCATTCCGTCTCCTTTTCCTGGTGGTTATTGTCC	475276	475335
ybaL_30	ATTTTTGGCCGGGAAAACCAAAATTACAGGTAATAGTTTATGACAATTTCATTGATGATG	475336	475395
ybaL_31	TTCATGAATAATTATTGAATTTTGCAGAAAAATGGAATTAGCTGCAAAAAAAGCACGGAT	475396	475455
topA_1	GCCTTACTGGCAACTTTGGATTTTGCATGCTAATAAAGTTGCGTATCGGATTTTATCAGG	1329119	1329178
topA_2	TACAGTGTGACGCTTTCGTCAATCTGGCAATAGATTTGCTTGACATTCGACCAAAATTCC	1329179	1329238
topA_3	GTCGTGCTATAGCGCCTGTAGGCCAAGACCTGTTAACTCAGTCACCTGAATTTTCGTGAA	1329239	1329298
topA_4	CAGAGTCACGACAAGGGGTTGATATCCGCAGAGAGCGAGTCCATATCGGTAACTCGTTGC	1329299	1329358
topA_5	CAGTGGAAGGTTTATCAACGTGCGACGCATTCCTGGAAGAATCAAATTAGGTAAGGTGAA	1329359	1329418
topA_6	TATGGGTAAAGCTCTTGTCATCGTTGAGTCCCCGGCAAAAGCCAAAACGATCAACAAGTA	1329419	1329478
topA_7	TCTGGGTAGTGACTACGTGGTGAAATCCAGCGTCGGTCACATCCGCGATTTGCCGACCAG	1329479	1329538
topA_8	TGGCTCAGCTGCCAAAAAGAGTGCCGACTCTACCTCCACCAAGACGGCTAAAAAGCCTAA	1329539	1329598
topA_9	AAAGGATGAACGTGGCGCTCTCGTCAACCGTATGGGGGTTGACCCGTGGCACAATTGGGA	1329599	1329658
topA_10	GGCGCACTATGAAGTGTTGCCTGGTAAAGAGAAGGTCGTCTCTGAACTGAAACAACTGGC	1329659	1329718
topA_11	TGAAAAAGCCGACCACATCTATCTCGCAACCGACCTTGACCGCGAAGGGGAAGCCATTGC	1329719	1329778
topA_12	ATGGCACCTGCGGGAAGTGATTGGGGGTGATGATGCGCGCTATAGCCGAGTGGTGTTTAA	1329779	1329838
topA_13	CGAAATTACTAAAAACGCGATCCGCCAGGCATTTAACAAACCGGGTGAGCTGAATATTGA	1329839	1329898
topA_14	TCGTGTTAATGCCCAGCAGGCGCGTCGCTTTATGGACCGCGTGGTGGGGTATATGGTTTC	1329899	1329958
topA_15	GCCGCTGCTATGGAAAAAGATCGCTCGTGGTCTGTCTGCCGGTCGTGTGCAGTCGGTGGC	1329959	1330018
topA_16	GGTTCGCCTGGTGGTCGAGCGTGAGCGTGAAATTAAAGCGTTCGTGCCGGAAGAGTTCTG	1330019	1330078
topA_17	GGAAGTCGATGCCAGCACGACCACGCCATCTGGTGAAGCGTTGGCGTTACAGGTGACTCA	1330079	1330138
topA_18	TCAGAACGACAAACCGTTCCGTCCGGTCAACAAAGAACAAACTCAGGCTGCGGTAAGTCT	1330139	1330198
topA_19	GCTGGAAAAAGCGCGCTACAGCGTGCTGGAACGTGAAGACAAACCGACAACCAGTAAACC	1330199	1330258
topA_20	TGGCGCTCCTTTTATTACCTCTACGCTGCAACAAGCTGCCAGCACCCGTCTTGGATTTGG	1330259	1330318
topA_21	CGTGAAAAAAACCATGATGATGGCGCAGCGTTTGTATGAAGCAGGCTATATCACTTACAT	1330319	1330378
topA_22	GCGTACCGACTCCACTAACCTGAGTCAGGACGCGGTAAATATGGTTCGCGGTTATATCAG	1330379	1330438
topA_23	CGATAATTTTGGTAAGAAATATCTGCCGGAAAGTCCGAATCAGTACGCCAGCAAAGAAAA	1330439	1330498
topA_24	CTCACAGGAAGCGCACGAAGCGATTCGTCCTTCTGACGTCAATGTGATGGCGGAATCGCT	1330499	1330558
topA_25	GAAGGATATGGAAGCAGATGCGCAGAAACTGTACCAGTTAATCTGGCGTCAGTTCGTTGC	1330559	1330618
topA_26	CTGCCAGATGACCCCAGCGAAATATGACTCCACGACGCTGACCGTTGGTGCGGGCGATTT	1330619	1330678
topA_27	CCGCCTGAAAGCACGCGGTCGTATTTTGCGTTTTGATGGCTGGACAAAAGTGATGCCTGC	1330679	1330738
topA_28	GTTGCGTAAAGGCGATGAAGATCGCATCTTACCAGCAGTTAATAAAGGCGATGCTCTGAC	1330739	1330798
topA_29	GCTCGTTGAACTTACACCAGCCCAGCACTTTACCAAGCCGCCAGCCCGTTTCAGTGAAGC	1330799	1330858
topA_30	ATCGCTGGTTAAAGAGCTGGAAAAACGCGGTATCGGTCGTCCGTCTACCTATGCGTCGAT	1330859	1330918
topA_31	CATTTCGACCATTCAGGATCGTGGCTACGTGCGAGTAGAAAATCGTCGTTTCTATGCGGA	1330919	1330978
topA_32	AAAAATGGGCGAAATCGTCACCGATCGCCTTGAAGAAAATTTCCGCGAGTTAATGAACTA	1330979	1331038
topA_33	CGATTTTACCGCGCAGATGGAAAACAGCCTCGACCAGGTGGCAAATCACGAAGCAGAGTG	1331039	1331098
topA_34	GAAAGCTGTACTGGATCACTTCTTCTCGGATTTCACCCAGCAGTTAGATAAAGCTGAAAA	1331099	1331158
topA_35	AGATCCGGAAGAGGGTGGTATGCGCCCGAACCAGATGGTTCTGACCAGCATTGACTGCCC	1331159	1331218
topA_36	GACTTGTGGTCGCAAAATGGGGATTCGCACAGCGAGCACCGGGGTATTCCTTGGCTGTTC	1331219	1331278
topA_37	TGGCTATGCGCTGCCGCCGAAAGAGCGTTGCAAAACCACCATTAACCTGGTGCCGGAAAA	1331279	1331338
topA_38	CGAAGTGCTGAACGTGCTGGAAGGCGAAGATGCTGAAACCAACGCGCTGCGCGCAAAACG	1331339	1331398
topA_39	TCGTTGCCCGAAATGCGGCACGGCGATGGACAGCTATCTCATCGATCCGAAACGTAAGTT	1331399	1331458
topA_40	GCATGTCTGTGGTAATAACCCAACCTGCGACGGTTACGAGATCGAAGAGGGCGAATTCCG	1331459	1331518
topA_41	CATTAAAGGTTATGACGGCCCGATCGTTGAGTGTGAAAAATGTGGCTCTGAAATGCACCT	1331519	1331578
topA_42	GAAAATGGGGCGTTTCGGTAAATACATGGCCTGCACCAACGAAGAGTGTAAAAACACACG	1331579	1331638
topA_43	TAAGATTTTACGTAACGGCGAAGTGGCACCACCGAAAGAAGATCCGGTGCCATTACCTGA	1331639	1331698
topA_44	GCTGCCGTGCGAAAAATCAGATGCTTATTTCGTGCTGCGTGACGGTGCTGCCGGTGTGTT	1331699	1331758
topA_45	CCTGGCTGCCAACACTTTCCCGAAATCGCGTGAAACGCGTGCGCCACTGGTGGAAGAGCT	1331759	1331818
topA_46	TTATCGCTTCCGCGACCGTCTGCCGGAAAAACTGCGTTATCTGGCCGATGCGCCACAGCA	1331819	1331878
topA_47	GGATCCGGAAGGTAATAAGACCATGGTTCGCTTTAGCCGTAAAACCAAACAGCAATATGT	1331879	1331938
topA_48	CTCTTCGGAAAAAGACGGAAAGGCGACTGGCTGGTCAGCATTTTATGTTGATGGCAAATG	1331939	1331998
topA_49	GGTTGAAGGAAAAAAATAACCTTTAATTCTGTCAGGTTTTTATAAACAAAGGGTCGCGAA	1331999	1332058
pykF_1	AACGCTGTTTTTGTTTTCCTTTTGGATTAATTTCAGCGTATAATGCGCGCCAATTGACTC	1732685	1732744
pykF_2	TTGAATGGTTTCAGCACTTTGGACTGTAGAACTCAACGACTCAAAAACAGGCACTCACGT	1732745	1732804

Name	Sequence	Start	End
pykF_3	TGGGCTGAGACACAAGCACACATTCCTCTGCACGCTTTTTCGATGTCACCTATCCTTAGA	1732805	1732864
pykF_4	GCGAGGCACCACCACTTTCGTAATACCGGATTCGCTTTCCGGCAGTGCGCCCAGAAAGCA	1732865	1732924
pykF_5	AGTTTCTCCCATCCTTCTCAACTTAAAGACTAAGACTGTCATGAAAAAGACCAAAATTGT	1732925	1732984
pykF_6	TTGCACCATCGGACCGAAAACCGAATCTGAAGAGATGTTAGCTAAAATGCTGGACGCTGG	1732985	1733044
pykF_7	CATGAACGTTATGCGTCTGAACTTCTCTCATGGTGACTATGCAGAACACGGTCAGCGCAT	1733045	1733104
pykF_8	TCAGAATCTGCGCAACGTGATGAGCAAAACTGGTAAAACCGCCGCTATCCTGCTTGATAC	1733105	1733164
pykF_9	CAAAGGTCCGGAAATCCGCACCATGAAACTGGAAGGCGGTAACGACGTTTCTCTGAAAGC	1733165	1733224
pykF_10	TGGTCAGACCTTTACTTTCACCACTGATAAATCTGTTATCGGCAACAGCGAAATGGTTGC	1733225	1733284
pykF_11	GGTAACGTATGAAGGTTTCACTACTGACCTGTCTGTTGGCAACACCGTACTGGTTGACGA	1733285	1733344
pykF_12	TGGTCTGATCGGTATGGAAGTTACCGCCATTGAAGGTAACAAAGTTATCTGTAAAGTGCT	1733345	1733404
pykF_13	GAACAACGGTGACCTGGGCGAAAACAAAGGTGTGAACCTGCCTGGCGTTTCCATTGCTCT	1733405	1733464
pykF_14	GCCAGCACTGGCTGAAAAAGACAAACAGGACCTGATCTTTGGTTGCGAACAAGGCGTAGA	1733465	1733524
pykF_15	CTTTGTTGCTGCTTCCTTTATTCGTAAGCGTTCTGACGTTATCGAAATCCGTGAGCACCT	1733525	1733584
pykF_16	GAAAGCGCACGGCGGCGAAAACATCCACATCATCTCCAAAATCGAAAACCAGGAAGGCCT	1733585	1733644
pykF_17	CAACAACTTCGACGAAATCCTCGAAGCCTCTGACGGCATCATGGTTGCGCGTGGCGACCT	1733645	1733704
pykF_18	GGGTGTAGAAATCCCGGTAGAAGAAGTTATCTTCGCCCAGAAGATGATGATCGAAAAATG	1733705	1733764
pykF_19	TATCCGTGCACGTAAAGTCGTTATCACTGCGACCCAGATGCTGGATTCCATGATCAAAAA	1733765	1733824
pykF_20	CCCACGCCCGACTCGCGCAGAAGCCGGTGACGTTGCAAACGCCATCCTCGACGGTACTGA	1733825	1733884
pykF_21	CGCAGTGATGCTGTCTGGTGAATCCGCAAAAGGTAAATACCCGCTGGAAGCGGTTTCTAT	1733885	1733944
pykF_22	CATGGCGACCATCTGCGAACGTACCGACCGCGTGATGAACAGCCGTCTCGAGTTCAACAA	1733945	1734004
pykF_23	TGACAACCGTAAACTGCGCATTACCGAAGCGGTATGCCGTGGTGCCGTTGAAACTGCTGA	1734005	1734064
pykF_24	AAAACTGGATGCTCCGCTGATCGTGGTTGCTACTCAGGGCGGTAAATCTGCTCGCGCAGT	1734065	1734124
pykF_25	ACGTAAATACTTCCCGGATGCCACCATCCTGGCACTGACCACCAACGAAAAAACGGCTCA	1734125	1734184
pykF_26	TCAGTTGGTACTGAGCAAAGGCGTTGTGCCGCAGCTTGTTAAAGAGATCACTTCTACTGA	1734185	1734244
pykF_27	TGATTTCTACCGTCTGGGTAAAGAACTGGCTCTGCAGAGCGGTCTGGCACACAAAGGTGA	1734245	1734304
pykF_28	CGTTGTAGTTATGGTTTCTGGTGCACTGGTACCGAGCGGCACTACTAACACCGCATCTGT	1734305	1734364
pykF_29	TCACGTCCTGTAATATTGCTTTTGTGAATTAATTTGTATATCGAAGCGCCCTGATGGGCG	1734365	1734424
spoT_1	GCAAATTGTTGGCAGACTGAACCTGATTTCAGTATCATGCCCAGTCATTTCTTCACCTGT	3760389	3760448
spoT_2	GGAGCTTTTTAAGTATGGCACGCGTAACTGTTCAGGACGCTGTAGAGAAAATTGGTAACC	3760449	3760508
spoT_3	GTTTTGACCTGGTACTGGTCGCCGCGCGTCGCGCTCGTCAGATGCAGGTAGGCGGAAAGG	3760509	3760568
spoT_4	ATCCGCTGGTACCGGAAGAAAACGATAAAACCACTGTAATCGCGCTGCGCGAAATCGAAG	3760569	3760628
spoT_5	AAGGTCTGATCAACAACCAGATCCTCGACGTTCGCGAACGCCAGGAACAGCAAGAGCAGG	3760629	3760688
spoT_6	AAGCCGCTGAATTACAAGCCGTTACCGCTATTGCTGAAGGTCGTCGTTAATCACAAAGCG	3760689	3760748
spoT_7	GGTCGCCCTTGTATCTGTTTGAAAGCCTGAATCAACTGATTCAAACCTACCTGCCGGAAG	3760749	3760808
spoT_8	ACCAAATCAAGCGTCTGCGGCAGGCGTATCTCGTTGCACGTGATGCTCACGAGGGGCAAA	3760809	3760868
spoT_9	CACGTTCAAGCGGTGAACCCTATATCACGCACCCGGTAGCGGTTGCCTGCATTCTGGCCG	3760869	3760928
spoT_10	AGATGAAACTCGACTATGAAACGCTGATGGCGGCGCTGCTGCATGACGTGATTGAAGATA	3760929	3760988
spoT_11	CTCCCGCCACCTACCAGGATATGGAACAGCTTTTTGGTAAAAGCGTCGCCGAGCTGGTAG	3760989	3761048
spoT_12	AGGGGGTGTCGAAACTTGATAAACTCAAGTTCCGCGATAAGAAAGAGGCGCAGGCCGAAA	3761049	3761108
spoT_13	ACTTTCGCAAGATGATTATGGCGATGGTGCAGGATATCCGCGTCATCCTCATCAAACTTG	3761109	3761168
spoT_14	CCGACCGTACCCACAACATGCGCACGCTGGGCTCACTTCGCCCGGACAAACGTCGCCGCA	3761169	3761228
spoT_15	TCGCCCGTGAAACTCTCGAAATTTACAGCCCGCTGGCGCACCGTTTAGGTATCCACCACA	3761229	3761288
spoT_16	TTAAAACCGAACTCGAAGAGCTGGGTTTTGAGGCGCTGTATCCCAATCGTTACCGCGTAA	3761289	3761348
spoT_17	TTAAAGAAGTGGTGAAAGCCGCGCGCGGCAACCGTAAAGAGATGATCCAAAAAATCCTCT	3761349	3761408
spoT_18	CTGAAATCGAAGGGCGTTTGCAGGAAGCGGGAATACCGTGCCGCGTCAGTGGTCGCGAAA	3761409	3761468
spoT_19	AGCATCTTTATTCGATTTACTGCAAAATGGTGCTCAAAGAGCAGCGTTTTCACTCAATCA	3761469	3761528
spoT_20	TGGACATCTACGCTTTCCGCGTGATCGTCAATGATTCTGACACCTGTTATCGCGTGCTGG	3761529	3761588
spoT_21	GCCAGATGCACAGCCTGTACAAGCCGCGTCCGGGCCGCGTGAAAGACTATATCGCCATTC	3761589	3761648
spoT_22	CAAAAGCGAACGGCTATCAGTCGTTGCACACCTCGATGATTGGCCCGCACAGCGTGCCGG	3761649	3761708
spoT_23	TTGAGGTCCAGATCCGTACCGAAGATATGGATCAGATGGCGGAGATGGGTGTTGCCGCGC	3761709	3761768
spoT_24	ACTGGGCTTATAAAGAGCACGGCGAAACCAGTACTACCGCACAAATCCGCGCCCAGCGCT	3761769	3761828
spoT_25	GGATGCAAAGCCTGCTGGAGCTGCAACAGAGCGCCGGTAGTTCGTTTGAATTTATCGAGA	3761829	3761888
spoT_26	GCGTTAAATCCGATCTCTTCCCGGATGAGATTTACGTTTTCACACCGGAAGGGCGCATTG	3761889	3761948
spoT_27	TCGAGCTGCCTGCCGGTGCAACGCCCGTCGACTTCGCTTATGCAGTGCATACCGATATCG	3761949	3762008
spoT_28	GTCATGCCTGCGTGGGCGCACGCGTTGACCGCCAGCCTTACCCGCTGTCGCAGCCGCTTA	3762009	3762068
spoT_29	CCAGCGGTCAAACCGTTGAAATCATTACCGCTCCGGGCGCTCGCCCGAATGCCGCTTGGC	3762069	3762128
spoT_30	TGAACTTTGTCGTTAGCTCGAAAGCGCGCGCCAAAATTCGTCAGTTGCTGAAAAACCTCA	3762129	3762188
spoT_31	AGCGTGATGATTCTGTAAGCCTGGGCCGTCGTCTGCTCAACCATGCTTTGGGTGGTAGCC	3762189	3762248
spoT_32	GTAAGCTGAATGAAATCCCGCAGGAAAATATTCAGCGCGAGCTGGATCGCATGAAGCTGG	3762249	3762308
spoT_33	CAACGCTTGACGATCTGCTGGCAGAAATCGGACTTGGTAACGCAATGAGCGTGGTGGTCG	3762309	3762368
spoT_34	CGAAAAATCTGCAACATGGGGACGCCTCCATTCCACCGGCAACCCAAAGCCACGGACATC	3762369	3762428
spoT_35	TGCCCATTAAAGGTGCCGATGGCGTGCTGATCACCTTTGCGAAATGCTGCCGCCCTATTC	3762429	3762488
spoT_36	CTGGCGACCCGATTATCGCCCACGTCAGCCCCGGTAAAGGTCTGGTGATCCACCATGAAT	3762489	3762548
spoT_37	CCTGCCGTAATATCCGTGGCTACCAGAAAGAGCCAGAGAAGTTTATGGCTGTGGAATGGG	3762549	3762608
spoT_38	ATAAAGAGACGGCGCAGGAGTTCATCACCGAAATCAAGGTGGAGATGTTCAATCATCAGG	3762609	3762668
spoT_39	GTGCGCTGGCAAACCTGACGGCGGCAATTAACACCACGACTTCGAATATTCAAAGTTTGA	3762669	3762728
spoT_40	ATACGGAAGAGAAAGATGGTCGCGTCTACAGCGCCTTTATTCGTCTGACCGCTCGTGACC	3762729	3762788
spoT_41	GTGTGCATCTGGCGAATATCATGCGCAAAATCCGCGTGATGCCAGACGTGATTAAAGTCA	3762789	3762848
spoT_42	CCCGAAACCGAAATTAATGTTTTATGAACCCAACACGTTATGCACGCATCTGCGAAATGC	3762849	3762908
hslU_1	AAATGGGGCCTTTCAGCCCCATCAAACAATGATGAAAATGATTGAACGCGATTATAGGAT	4099848	4099907
hslU_2	AAAACGGCTCAGATCTTCATCTGCCACCAACGCATCCAGATGTTTGCTCACATAATCTGC	4099908	4099967
hslU_3	GTCAATAGTGATATTTTGACCGCTTAAATCGCTGGCGTCGTAGGAAATCTCTTCCATTAA	4099968	4100027
hslU_4	ACGCTCCAGAACAGTGTGTAAACGACGAGCACCGATGTTTTCGGTAGATTCGTTCACCTG	4100028	4100087
hslU_5	CCATGCCGCTTCCGCGATGCGTTTAATACCGGAGTCGGTAAACTCGATATTTACGCCTTC	4100088	4100147
hslU_6	AGTCGCCATCAGTGCTTTGTACTGCACGGTGATAGAGGCATTCGGCTCGGTCAGAATACG	4100148	4100207
hslU_7	CTCGAAGTCGCTGGTGGTCAGCGCCTGCAGTTCAACGCGGATTGGCAGACGACCTTGCAG	4100208	4100267
hslU_8	TTCCGGGATCAGGTCAGACGGTTTCGCAATCTGGAACGCGCCAGAAGCGATAAACAGAAT	4100268	4100327
hslU_9	GTGGTCAGTTTTGACCATCCCGTGTTTGGTGGAAACGGTGCAACCTTCTACCAGCGGCAG	4100328	4100387
hslU_10	CAGGTCACGCTGAACGCCTTCACGAGAAACATCCGGACCGGAAGACTCGCCGCGCTTACA	4100388	4100447
hslU_11	GATTTTGTCGATTTCGTCGATAAACACGATCCCGTGCTGCTCAACAGCGTCGATAGCGTC	4100448	4100507
hslU_12	TTGCTTCAGCTCTTCCGGGTTCACCAGTTTCGCCGCTTCTTCTTCAATCAGCAGCTTCAT	4100508	4100567
hslU_13	GGCGTCTTTGATTTTCAGCTTACGCGCTTTTTGCTTCTGGCCGCCCAGGTTCTGGAACAT	4100568	4100627
hslU_14	GGACTGCAGCTGGCTGGTCATCTCTTCCATGCCCGGAGGAGCCATAATTTCAACGCCCAT	4100628	4100687
hslU_15	CGGTGCTGCGGCAAGATCGATCTCGATTTCTTTGTCATCAAGCTGGCCTTCACGCAGTTT	4100688	4100747
hslU_16	TTTGCGGAATGCCTGACGAGCAGCGGACGGTTCCTGCTGCTGTTCGGTCTGTCCCCAGTT	4100748	4100807

Name	Sequence	Start	End
hslU_17	GTTTTTAGCAGGTGGGATCAGCACGTCGAGAATACGTTCTTCTGCCAGTTCTTCAGCGCG	4100808	4100867
hslU_18	ATAACGGTTTTTCTCGATAGCCTGGACGCGTACCATTTTCACGGCGGCATCGGTCAGATC	4100868	4100927
hslU_19	GCGAATAATAGAATCCACTTCCTTACCGACGTAGCCCACTTCGGTGAATTTGGTCGCTTC	4100928	4100987
hslU_20	AACTTTGATGAACGGCGCATTCGCCAGCTTAGCCAGACGACGGGCGATTTCAGTTTTACC	4100988	4101047
hslU_21	GACACCGGTCGGGCCGATCATCAGGATATTTTTCGGGGTCACTTCATGGCGCAGCTCTTC	4101048	4101107
hslU_22	GTTGAGCTGCATGCGACGCCAGCGGTTACGCAGAGCAATCGCCACAGAACGCTTGGCGTT	4101108	4101167
hslU_23	GTCCTGGCCGATGATGTGCTTATCCAGTTCGCTGACGATTTCGCGTGGGGTCATTTCAGA	4101168	4101227
hslU_24	CATGGGAGATCCTTACGCTTTGTAGCTTAATTCTTCGATGGTGTGGAAATGGTTGGTATA	4101228	4101287
hslU_25	GATGCAAATGTCGCCTGCAATATCCAACGCCTTTTCAGCAATTTCACGGGCGCTAAGTTC	4101288	4101347
hslU_26	AGTGTTTTCTAACAGCGCGCGCGCCGCAGCCTGGGCGTAAGGGCCGCCGGAGCCGATAGC	4101348	4101407
hslU_27	AATAAGATCGTTTTCTGGCTGCACCACGTCACCGTTACCGGTGATGATAAGCGATGCAGT	4101408	4101467
hslU_28	TTCATCCGCGACTGCCAGCAGTGCTTCAAGTTTGCGCAGCATGCGATCGGTACGCCAGTC	4101468	4101527
hslU_29	TTTTGCCAGCTCAACGGCGGCTTTGACCAGATGGCCCTGATGCATTTCCAGTTTACGTTC	4101528	4101587
hslU_30	AAACAGTTCGAACAGCGTAAAAGCATCCGCAGTACCGCCCGCAAAGCCCGCGATGACTTT	4101588	4101647
hslU_31	GTCGTTGTACAGACGGCGGACCTTTTTCACGTTGCCTTTCATTACGGTATTGCCCAACGT	4101648	4101707
hslU_32	GGCCTGACCATCACCAGCGATGACCACATGGCCGTTACGGCGTACGCTTACTATAGTTGT	4101708	4101767
hslU_33	CACGAGCTGACCCCTTGGTTACGAATACAGAGTACAAACCCCGTACAAAAGTACGGGGCA	4101768	4101827
hslU_34	TAATGCAATTATAGATGGGGGGGATTTTGAGGGTTTCAACCCCCGGCGGCGAGCCGAATG	4101828	4101887
fabR_1	GCCGGGGCCGGAACCTATTACTATGGCATCGTAATCGTAGGAATGTGGCATGGTAGGGCT	4140601	4140660
fabR_2	TACCTGTTCTTATACATAAAAGCAACAGAATGGTAACATTTTATCGCGGGTAAGCCAATT	4140661	4140720
fabR_3	GATCCCCGTCATTTATCTGGCTATATCCTGAGCGGCCTTTGCTTTGTCTGTTTCTTACTT	4140721	4140780
fabR_4	TTGCCCTGACGTTTTATTGGATTTTTATCGACGATACTCTCCGTTTAAGCGGCAGGTTTC	4140781	4140840
fabR_5	CGCTGTACGTAAAAGAACCGGCCAAAGAATTGCAGTAAATATGTTTTATTGCGTTACCGT	4140841	4140900
fabR_6	TCATTCACAATACTGGAGCAATCCAGTATGTTCATTCTCTGGTATAGTGCCAGCAGTACT	4140901	4140960
fabR_7	TTTGGCAAGGATTCAGACATCGTGATGGGCGTAAGAGCGCAACAAAAAGAAAAAACCCGC	4140961	4141020
fabR_8	CGTTCGCTGGTGGAAGCCGCATTTAGCCAATTAAGTGCTGAACGCAGCTTCGCCAGCCTG	4141021	4141080
fabR_9	AGTTTGCGTGAAGTGGCGCGTGAAGCGGGCATTGCTCCCACCTCTTTTTATCGGCATTTC	4141081	4141140
fabR_10	CGCGACGTAGACGAACTGGGTCTGACCATGGTTGATGAGAGCGGTTTAATGCTACGCCAA	4141141	4141200
fabR_11	CTCATGCGCCAGGCGCGTCAGCGTATCGCCAAAGGCGGGAGTGTGATCCGCACCTCGGTC	4141201	4141260
fabR_12	TCCACATTTATGGAGTTCATCGGTAATAATCCTAACGCCTTCCGGTTATTATTGCGGGAA	4141261	4141320
fabR_13	CGCTCCGGCACCTCCGCTGCGTTTCGTGCCGCCGTTGCGCGTGAAATTCAGCACTTCATT	4141321	4141380
fabR_14	GCGGAACTTGCGGACTATCTGGAACTCGAAAACCATATGCCGCGTGCGTTTACTGAAGCG	4141381	4141440
fabR_15	CAAGCCGAAGCAATGGTGACAATTGTCTTCAGTGCGGGTGCCGAGGCGTTGGACGTCGGC	4141441	4141500
fabR_16	GTCGAACAACGTCGGCAATTAGAAGAGCGACTGGTACTGCAACTGCGAATGATTTCGAAA	4141501	4141560
fabR_17	GGGGCTTATTACTGGTATCGCCGTGAACAAGAGAAAACCGCAATTATTCCGGGAAATGTG	4141561	4141620
fabR_18	AAGGACGAGTAATGAAACAAGCAAATCAAGATAGAGGTACGCTGCTGCTGGCGTTAGTTG	4141621	4141680
iclR_1	TCTATTGCCACTCAGGTATGATGGGCAGAATATTGCCTCTGCCCGCCAGAAAAAGTCAGC	4201680	4201739
iclR_2	GCATTCCACCGTACGCCAGCGTCACTTCCTTCGCCGCTTTAATCACCATTGCGCCAAACT	4201740	4201799
iclR_3	CGGTCACGCGGTCATCGGTAATACGTGAAATCGGTCCGGAAATAGAAATTGCGGCAAACG	4201800	4201859
iclR_4	GTTCACGGTGCTCATCGAAAATACACGCTGCAAGGCAACGTAGCCCCAGCGCATGTTCCT	4201860	4201919
iclR_5	CATCGTCAAATGAATAACCCCGTTTGCGCGTTTGGGCGAGATCTTCTTTTAAATGCACAG	4201920	4201979
iclR_6	GAGACACCAGCGTTGCGTGGGTATAGGCATGTAACCCTTTGCGGTGCAGCAGCTTCGTCA	4201980	4202039
iclR_7	CCTGTTCTTCGCTCAGTTGGGCTAAAAAGGCTTTACCTGCACCGGAAGCGTGCATCGGCA	4202040	4202099
iclR_8	ATTTACCGCCGATAGGCGCGGACATTCGCATCAGATGCGTACACTGTACCTGGTCGATAA	4202100	4202159
iclR_9	TAATCGCTTCGTGATCGCTTTGATCAAGCACCGCCATATTGACCGTTTCGCCAGACTCTT	4202160	4202219
iclR_10	CCATTAAATTGCGCAGGATAGGGTGAACAATCGCTAACAAATTACGGCTCTGGAGAAAGC	4202220	4202279
iclR_11	TGCTGCCGACCATAAAGGCATGTGCGCCGATTGCCCAATGTCCCAGTTCGCCGACCTGAC	4202280	4202339
iclR_12	GCACGAAACCCTGCTGTTGCATTGTGGTTAGCAGGCGGTGGGTCGTGGAATTGGGTAACC	4202340	4202399
iclR_13	CGGCTTGTTGCGCCAGTTCCGTGAGTGCCACACTGCCATTGGATTCGGCAATCCACTCCA	4202400	4202459
iclR_14	GTAATTTCAGGCCACGCGTTAAAGACTGAACCTGTCCAGTCGCTGGTGCGGTGGCAACGG	4202460	4202519
iclR_15	CGGGTTTTCTGCCGCGTTTCGCGGGAATGGGTGCGACCATGACAGTCTCCTTTTTCTGTA	4202520	4202579
iclR_16	TCGTGGAAATCATTTTCATTTTTATTGTTAGCTAATGCAATAGTTGCTGAACTGATCCGA	4202580	4202639
iclR_17	TGAGTTAATGTTGAACAAATCTCATGTTGCGTGGTGGTCGCTTTTACCACAGATGCGTTT	4202640	4202699
nadR_1	CTTAGCGTGTTCGACGACTTATAATGAGGAATACGGAGGGAGATATGTCGTCATTTGATT	4615485	4615544
nadR_2	ACCTGAAAACTGCCATCAAGCAACAGGGCTGCACGCTACAGCAGGTGGCTGATGCCAGCG	4615545	4615604
nadR_3	GTATGACCAAAGGGTATTTAAGCCAGTTACTGAATGCCAAAATCAAAAGCCCCAGCGCGC	4615605	4615664
nadR_4	AAAAGCTGGAGGCGTTGCACCGTTTTTTGGGGCTTGAGTTTCCCCGGCAGAAGAAAACCA	4615665	4615724
nadR_5	TTGGTGTGGTATTCGGTAAGTTCTACCCGCTGCATACCGGACATATCTACCTTATCCAGC	4615725	4615784
nadR_6	GCGCCTGTAGCCAGGTTGACGAACTGCATATCATTATGGGTTTTGACGATACCCGCGATC	4615785	4615844
nadR_7	GCGCGTTGTTTGAAGACAGCGCTATGTCGCAGCAGCCCACCGTGCCGGATCGTCTGCGCT	4615845	4615904
nadR_8	GGTTATTACAAACTTTTAAATATCAGAAAAATATTCGCATTCATGCTTTCAACGAAGAGG	4615905	4615964
nadR_9	GCATGGAGCCGTATCCGCACGGCTGGGATGTGTGGAGCAACGGCATCAAAAAGTTTATGG	4615965	4616024
nadR_10	CTGAAAAGGGGATTCAGCCGGACCTGATCTACACCTCGGAAGAAGCCGATGCGCCACAGT	4616025	4616084
nadR_11	ATATGGAACATCTGGGGATCGATACGGTGCTGGTCGATCCGAAACGTACCTTTATGAGTA	4616085	4616144
nadR_12	TCAGCGGTGCGCAGATCCGCGAAAACCCGTTCCGCTACTGGGAATATATTCCTACGGAAG	4616145	4616204
nadR_13	TGAAGCCGTTCTTTGTACGTACCGTGGCGATCCTTGGTGGCGAGTCGAACGGTAAATCCA	4616205	4616264
nadR_14	CCCTGGTAAACAAACTTGCCAATATCTTCAATACCACCAGTGCGTGGGAATATGGTCGCG	4616265	4616324
nadR_15	ATTATGTCTTTTCACACCTCGGCGGTGATGAGATCGCATTGCAGTATTCCGATTACGATA	4616325	4616384
nadR_16	AAATCGCGCTGGGCCACGCACAATACATTGATTTTGCAGTGAAATATGCCAATAAAGTGG	4616385	4616444
nadR_17	CGTTTATTGACACTGATTTTGTCACTACCCAGGCGTTCTGCAAAAAGTACGAAGGGCGTG	4616445	4616504
nadR_18	AGCATCCGTTCGTACAGGCGTTGATTGATGAATACCGTTTCGATCTGGTGATCCTGCTGG	4616505	4616564
nadR_19	AGAACAACACGCCGTGGGTGGCGGATGGTTTACGCAGCCTCGGCAGTTCGGTGGATCGCA	4616565	4616624
nadR_20	AAGAGTTCCAGAACTTGCTGGTGGAGATGCTGGAAGAGAACAATATCGAATTCGTGCGGG	4616625	4616684
nadR_21	TTGAAGAGGACGATTATGACAGCCGTTTCCTGCGCTGCGTGGAGCTGGTGCGGGAGATGA	4616685	4616744
nadR_22	TGGGGGAGCAGAGATAACCGCGATGAAACGGCTCAAAGGCGAGGTATAAAATAAGTTTTT	4616745	4616804

All sequences were ordered as xGen Lockdown probes with a 5′ biotin tag from Integrated DNA Technologies. Start and end are the positions where the first and last base map to in the *E. coli* REL606 genome (GenBank: NC_012967.1).

Table S3. Blocker sequences

Name	Sequence
Universal Blocker	AATGATACGGCGACCACCGAGATCTACACTCTTTCCCTACACGACGCTCTTCCGATCT
Degenerate Sample Barcode Blocker	CAAGCAGAAGACGGCATACGAGAT**NNNNNN**GTGACTGGAGTTCAGACGTGTGCTCTTCCGATCT

Red bases anneal to the sample barcodes. They were synthesized with a mixture of all four bases so that one blocking oligo could be used in pulldowns in which multiple different sample barcodes were present.